INSTITUTO SUPERIOR DE ENGENHARIA DE LISBOA

Área Departamental de Engenharia de Electrónica e Telecomunicações e de Computadores

Flexible RFID tag for bottle labelling

David da Costa Guilherme Cheis Rodrigues

Licenciado

Dissertação para obtenção do Grau de Mestre
em Engenharia Eletrónica e Telecomunicações

Orientadores : Prof. Doutor Pedro Pinho
Prof. Doutor Carlos Mendes

Júri:

Presidente: Prof. Doutor António Serrador

Vogais: Prof. Doutor Custódio Peixeiro
Prof. Doutor Pedro Pinho

setembro, 2021

Acknowledgments

First of all I would like to thank both my supervisors, Prof. Pedro Pinho and Prof. Carlos Mendes, for all the support provided during the realization of this dissertation, for all the constant good mood and ease and for all the knowledge they shared. To them, a special thank you.

I would also like to thank the Instituto de Telecomunicações de Aveiro, for all the material and equipment provided and for the fabrication of the antennas developed in this work.

To my family, for all their support during all my academic course, and for always wanting me to be and do better.

Last but not least, a thank you to my close and lifelong friends I made during this journey. Without you college would not have been so joyful. Thanks also to my co-worker Ruben for his help during our work free time.

Abstract

Radio frequency identification technology is increasingly being used as a solution for identification services and for retail product inventory control. However, it remains a major challenge to fully replace existing technologies with RFID due to the unavailability of antennas applicable on any type of product. An example of this difficulty is the use of these antennas on bottles. The presence of a liquid drastically changes the performance and adaptation of the antennas, making them non-functional for this type of products if they were not specifically designed for it.

The subject of this dissertation consists in the development of a flexible RFID antenna that works when applied to a bottle with liquid. For this purpose, antenna size reduction techniques and impedance matching techniques between the antenna and the microchip are studied in order to substantially reduce the size of an already operational antenna and make it functional for a bottle filled with liquid.

RFID tags were built to work in free space and then modified to be applied to bottles with liquid. The tags' size was reduced to one third of their original size. The results obtained, from tests carried out to achieve the maximum reading distances of the antennas, show that they perform well when applied to the environment for which they were designed. It is also perceptible in these tests that changes in the environment such as changing the liquid inside the bottle reflect changes in the performance of the antennas making them non-functional.

Keywords: Radio Frequency Identification, antenna, tag, RFID tags on bottles, impedance matching, antenna size reduction

Resumo

A tecnologia de identificação por radiofrequência (RFID) tem vindo cada vez mais a ser utilizada como solução para serviços de identificação e para controlo de inventário de produtos de retalho. Contudo, continua a ser um grande desafio substituir totalmente as tecnologias existentes por RFID devido à difícil generalização de antenas para qualquer tipo de produto. Um exemplo desta dificuldade é a utilização destas antenas em garrafas. A presença de um líquido altera drasticamente o desempenho e adaptação das antenas tornando-as não funcionais para este tipo de produtos caso não tenham sido dimensionadas especificamente para tal.

O tema desta disertação consiste no desenvolvimento de uma antena RFID flexível que funcione quando aplicada a uma garrafa com líquido. Para tal são estudadas técnicas de redução de tamanho de antenas e técnicas de adaptação de impedânica entre a antena e o microchip nela presente, com o objetivo de se reduzir substancialmente o tamanho de uma antena já operacional e torná-la funcional para uma garrafa com líquido.

Foram construídas tags RFID para funcionamento em espaço livre e posteriormente modificadas para aplicar em garrafas com líquido. Foi conseguido reduzi-las para um terço dos seus tamanhos originais. Os resultados obtidos, provenientes de testes efetuados para lograr as distâncias máximas de leitura das antenas, demonstram que estas apresentam um bom desempenho quando aplicadas ao ambiente para o qual foram dimensionadas. É também percéptível nestes testes que alterações no ambiente como alterar o líquido no interior da garrafa refletem alterações na performance das antenas tornando-as não funcionais.

Palavras-chave: Identificação por radiofrequência, antena, tag, tags RFID em garrafas, *matching* de impedânica, redução de tamanho de antena

Contents

List of Figures

List of Tables

Acronyms

ANACOM	Autoridade Nacional de Comunicações
EPC	Electronic Product Code
IBM	International Business Machines Corporation
IC	Integrated Circuit
IFA	Inverted F Antenna
IFF	Identification Friend or Foe
ITF	Interrogator-Talks-First
NFC	Near Filed Communication
RADAR	Radio Detection and Ranging
RF	Radio Frequency
RFID	Radio Frequency IDentification
UHF	Ultra High Frequency

1

Introduction

1.1 Radio frequency identification

Radio Frequency IDentification (RFID) refers to a technology where digital data encoded in RFID tags is captured by a reader via radio waves. This is an automatic identification technology and is mainly used for identification of people or objects. A tag is attached to what is wanted to be tracked or identified and when it passes near a reader the tag responds to the reader's signal with information of the associated item. Technologies like barcode, magnetic strip, fingerprint, optical recognition are also identification technologies, however RFID uses automatic data capture systems which increases its efficiency compared to other technologies [1].

RFID technology started with the need for identification of aircrafts during the World War II [2]. Radio Detection and Ranging (RADAR) technology was used to detect incoming aircrafts by emitting radio waves and detecting the reflected waves. However, it was only possible to detect the presence of an aircraft without being able to distinguish which country it was from. Given this problem, RADAR developer Alexander Watson-Watt also developed the first system capable of identifying allied aircrafts, called Identification Friend or Foe (IFF) [3]. In this system, transmitters were installed in all allied aircrafts, whose function was to emit a broadcast signal identifying the aircraft as a "friend" after receiving the signal from RADAR. This is the fundamental idea on which RFID known nowadays is based. In 1948, the paper "Communications by Means of Reflected Power" was published and can be considered as the birth of the RFID technology.

In 1973 the first RFID patents were created, where RFID tags were created with rewritable memory and passive RFID transponders were firstly used to unlock doors without the need of a key. Later, RFID systems began to be used in tool gate control systems and to locate people inside buildings, such as hospital patients or company employees. The UHF RFID system was patented by International Business Machines Corporation (IBM) in the 1990s. Since then, measures and protocols have been created to make this technology legislated worldwide, contributing to its diverse use and expansion.

Just recently, the RFID systems conquered an increasing area of intervention in society, either for product identification or inventory, either associated with passive sensors for location or sensors that measure temperature and humidity [4].

The use of RFID on inventory control is best understood by analysing how we have been controlling inventory with bar codes over the past decades. The bar code technology in use today requires every case and pallet to be scanned in all inventory phases (shipping, receiving, etc). Therefore the labor and process time involved in bar code based inventory control becomes a major drawback to further increase efficiency and speed. Other main advantage that RFID tags have is the fact that they become a small database of information regarding the product specifications and/or inventory cycle, so issues like traceability and expiration dates can be accurately tracked or estimated more efficiently [5].

As resourceful as the bar code technology is, RFID provides a better method that eliminates the requirement for line of sight scanning. RFID readers can be strategically placed on the production or inventory chains so that when the products pass near them, the energized tag reflects back the encoded data of its associated product even if it is not in line of sight with the reader.

To identify an object with RFID the Electronic Product Code (EPC) was created. These codes, defined and created by the EPCGlobal organization, are designed to be unique among all physical objects and all categories of physical objects in the world [6].

1.2 Motivation and goal

However there are a wide range of different materials where RFID tags can be applied and the antennas behave differently dependently on the material that they are implanted on. In this sense the exploration of new supports (paper, cork, fabric) for this type of systems is fundamental to continue exploring new applications using this type of sensors.

Although the RFID has a lot of advantages when comparing to the bar code technology,

it also has some handicaps. The development of versatile and low-cost tags for the labelling of bottles remains a major challenge due to the unsatisfactory performance of the antennas when in presence of different liquids.

Thus, the main objective of this dissertation is to build a RFID tag which is embedded in a flexible material that allows it to be easily integrated on a bottle. This requires overcoming challenges such as getting the antenna to perform reasonably well in the presence of glass and water and in a bent position when applied on a bottle. It is also important to take into account the total dimensions of the antenna. The smaller and more discreet it is the better, allowing for an easy installation on the bottle.

A functional free-space RFID antenna is first studied and tested in CST Studio software in order to match it to a RFID microchip. Afterwards, simulations and adjustments are carried in order to adapt the antenna to work on a bottle and later on a bottle with liquid. Finally, RFID tag antennas are built and several tests are performed to stress the antennas' functionality in electromagnetic controlled and uncontrolled environments and for different bottles and liquids, retrieving conclusions and results of the antennas' performance.

1.3 Organization

This document is divided into six chapters, including this introductory chapter:

- Chapter 2 - RFID Principles: In this chapter an introductory explanation and overview is made about the principles of the RFID technology. The state of the art of the technology is also addressed;
- Chapter 3 - Free Space RFID tag antennas: Techniques for impedance matching and antenna size reduction are contemplated on this chapter and a thorough study of an RFID antenna is made;
- Chapter 4 - RFID tag antennas appled on bottles: In this chapter it is explained all the processes and simulations made to achieve an antenna theoretically functional for a bottle full of water;
- Chapter 5 - Tag range measurement: The dissertation practical measurements and results are demonstrated in this chapter;
- Chapter 6 - Conclusions: This chapter summarizes this dissertation conclusions. Future work is also discussed.

2

RFID principles

In this chapter is described the state of the art of RFID technology. Firstly an overview of the different types of frequency bands is given, comparing reading ranges and use cases. After is an approach to the tag's components and classes followed by an explanation of the operating mode of RFID systems. Aftermost there is a brief description of the protocol used in UHF RFID system regarding this dissertations objectives, ISO 18000-6C.

2.1 RFID technology

Radio frequency identification is a form of wireless communication that incorporates the use of electromagnetic waves in the radio frequency portion of the electromagnetic spectrum to uniquely identify an object, animal or person. This technology can bring a great deal of advantages in a wide range of areas like healthcare, manufacturing, inventory management and control, shipping, retail sales and home use.

A RFID system is formed by two components, a reader and a tag, as it can be seen on figure 2.1. The reader, also designated as interrogator or scanner, may have multiple antennas that are responsible for sending and receiving radio waves. It is responsible for powering the tag, in some cases, and communicating with it. The tag is composed by a simple silicon microchip and an antenna that captures the signal transmitted by the reader and transfers back information [4] [7]. Both these components are described in more detail further ahead.

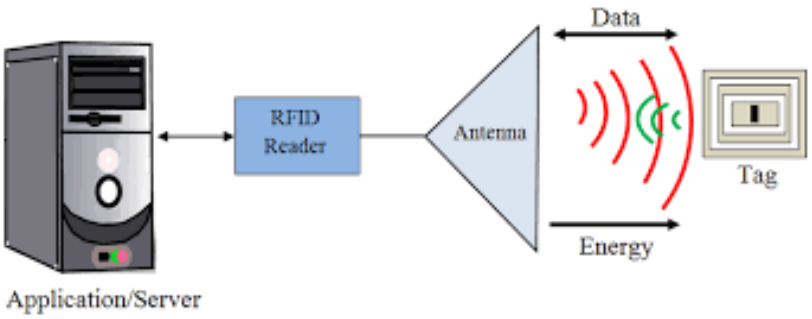

Figure 2.1: RFID system representation. (extracted from [8].)

The RFID systems can be categorized in three different frequency operating ranges. Each radio frequency has its own read distance, power requirements and performance [9]. Although these ranges can vary within a certain range from country to country, depending on each country's telecommunications regulator, the typical operating frequencies are:

- **Low Frequency (LF)**: These systems operate in the frequency ranges from 30 kHz to 300 kHz. Reading range can go up to 15 cm. In spite of the fact that their reading ranges are shorter and their data reading rate is slower than other technologies, this one performs better in presence of metal or liquid substances. It's common use cases are access control, livestock tracking, and other applications where short reading ranges are acceptable;
- **High Frequency**: Operating in a range between 3 MHz to 30 MHz, systems using these frequencies can achieve reading distances from 10 cm to 1 m. These types of RFID are currently being used in data transfer applications like Near Filed Communication (NFC), which allows to transfer multimedia content and other type of data between cellphones. Other applications are proximity card payments and hotel room keying [9];
- **Ultra-High Frequency**: RFID UHF systems operate in a frequency range between 300 MHz to 3 GHz and can provide reading distances up to 12 m, theoretically [9]. It's the type of system that is more sensitive to interference from metal, liquids and electromagnetic signals. Still, the tags of this frequency type are the cheapest to produce and for this reason, and also its high reading range, they are the most commonly used in retail inventory tracking and other areas where large volume of tags are needed.

Immediately below it's table 2.1 that summarizes the RFID frequency system types, frequency and reading ranges and the typical applications where they're used.

Table 2.1: Summary of RFID technology types.

Technology Type	Frequency Range	Reading Range	Use cases
LF	30 - 300 [KHz]	10 - 15 [cm]	Access Control / Livestock tracking
HF	3 - 30 [MHz]	0.1 - 1 [m]	Data Transfer Applications
UHF	0.3 - 3 [GHz]	12 [m]	Retail Inventory Management / Shipping

Althought the UHF RFID is the frequency band where the signals deteriorate more from interference sources, also because it's a used radio mobile frequency, it's definitely the one that adds the most values in inventory tracking. In this sense, the developed tag on this dissertation is a UHF RFID tag [7].

2.2 Tag types

There are primarily three types of tags that a RFID system can use: active, passive and semi-passive tags. The main difference between them is the source of internal powering. RFID tags contain at least three parts: an integrated circuit that stores and processes information and that modulates and demodulates radio frequency signals, a means of collecting DC power from the incident reader signal and an antenna for receiving and transmitting the tag's signal. The choice of which type of tag to use is dependent on the use case or application of the RFID system [10]. Below is a more detailed explanation of tag types.

- **Active Tag**: This kind of tags have an own battery supply that it's used to power up the internal circuits (microship) and the backscattering signals. Since it has it's own power supply, the transmitted signal from these tags can be read at higher distances since it does not only rely on the energy derivative from the reader's signal. However these tags are expensive, mainly due to the baterry prices, and require maintenance such as battery replacement;

- **Passive Tag**: Unlike the previous tag type these don't have a self power supply. These tags rely on the energy of the transmitting reader's signal to power up their microship and backscatter the response signal with the requested information. Due to this fact their reading range is lower when compared to an active tag. On the other hand their manufacturing prices are much cheaper and don't require maintenance;

- **Semi-passive Tag**: This type of tag have also a battery for energy supply. Although, and dissimilar to active tags, this tag's battery is only used to feed the internal circuits and it only occurs when the antenna receives a signal from the reader. A semi-passive tag still requires the energy from the reader's signal to be able to transmit its backscatter signal.

In the figures 2.2 and 2.3 below an example of an active and a passive RFID tag can be seen.

Figure 2.2: Active RFID tag.

Figure 2.3: Passive RFID tag.

Tags can also be classified by their memory type:

- **Read only**: This tag's data can only be written one time, during the manufacturing process, and it can't be changed. Since they can be read multiple times, these memory type tag's are very usefull on commercial applications like inventory.
- **Read-Write**: The data of these tags can be changed many times, which can make them a good type choice if used in applications that require information change and/or update regularly.

Use cases and applications may have different or similar uses for tags where some are successful using active ones and others using passive and semi-passive types. The versatility of the tags can be the deciding factor in which tag type to use in an operation. Nevertheless, since the purpose of this dissertation is to design and implement a tag on a bottle labelling, only the passive tag type will be considered. The tag's memory type isn't a relevant concern since either categories work for testing purposes.

2.3 Operating methods

Passive tag does not have its own power source. So in order to achieve power transfer from the reader to the tag two essential RFID strategies exist: inductive coupling and

backscatter wave coupling. These two approaches take advantage of the electromagnetic properties associated with an Radio Frequency (RF) antenna, the near and far field. For electrically small antennas, the near field area dimension is approximately until $d << \frac{\lambda}{2\pi}$, while the far field appears when distance is superior to 2λ. Both these methods can provide enough power to sustain a remote tag's operation [7].

2.3.1 Inductive coupling

The near-field coupling is based on Faraday's principle of magnetic induction [4]. When the reader charges its antenna coil with an alternating current a magnetic field is generated. Part of this emitted field penetrates the tag's antenna coil and a voltage is produced by induction.

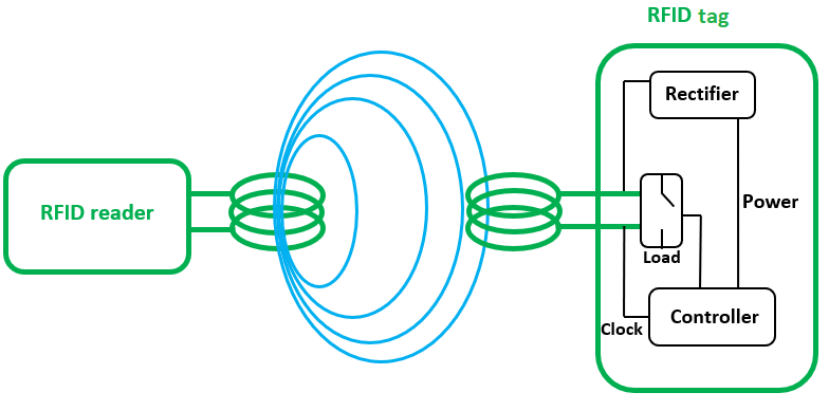

Figure 2.4: Inductive Coupling operating mode.

This voltage passes through a rectifier, as it can be seen in figure 2.4 and its used to power the microchip present in the tag. A signal can be encoded as variations in the magnetic field applying a load that's present in the microchip just like the rectifier. This signal can transmit the tag's identification for instance. One of its limitations is that the energy for inductive coupling drops rapidly with distance, having a ratio of $\frac{1}{d^3}$ where d the distance between the reader and the tag [4].

2.3.2 Backscatter coupling

The far field region is the most important in the backscatter coupling as it determines the antenna's radiation pattern. If the antenna on the tag is designed with precise dimensions to be tuned at a certain frequency it captures the electromagnetic waves transmitted by the reader as potential difference that appears on the arms of it [7]. Despite that, the antenna must also be matched with the impedance of the microchip so

that it won't reflect some of the signal's energy back instead of receiving the fullest. The antennas being dimensioned in this dissertation are design to work in UHF systems where backscatter coupling is the used method.

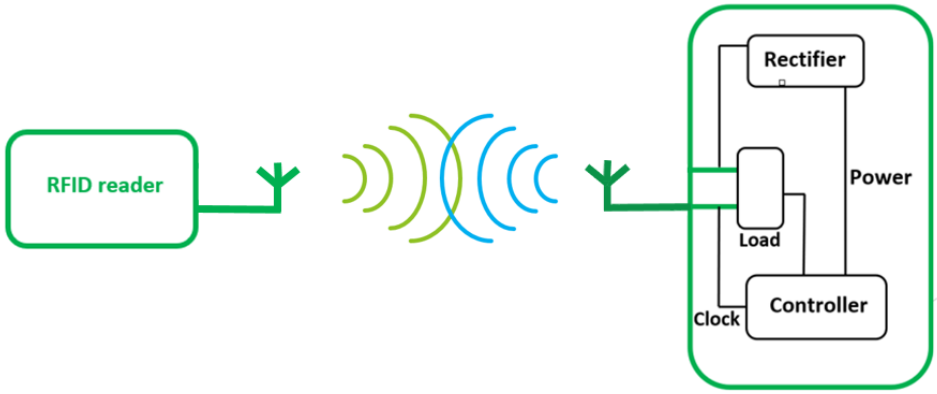

Figure 2.5: Backscatter Coupling operating mode.

In the figure 2.5 is exhibited the backscatter operating mode previously described. The reading ranges of this method can differ with the sensitivity of the reader to detect the backscatter signal or the amount of energy that reaches the tag through the reader's transmission.

Data exchange between reader and tag in a RFID system can employ various modulation and coding schemes. The standards for modulations and encodings set for this type of coupling and UHF RFID systems are described in the ISO 18000-6C explained in the next section.

2.4 ISO protocol 18000-6C

ISO Protocol 18000-6C is an arrangement that allows to connect and establish communication between two systems. It describes the communication standards set for Interrogator-Talks-First (ITF) RFID readers and tags [6]. This protocol was firstly developed and put into practice by EPC Global Organization, as the EPC Gen 2, and later the International Organization for Standardization (ISO) approved and adopted it as ISO Protocol 18000-6C so that it is standardized worldwide [11] [12]. Typically, this protocol uses two main frequency bands: 902-928 MHz and 865-868 MHz. However, the use of these frequency bands is always regulated by the telecommunications regulator in each country, so the frequency of the UHF RFID technology may change from

country to country. The world map represented in figure 2.6 can give a perception of how these bands are scattered around the world.

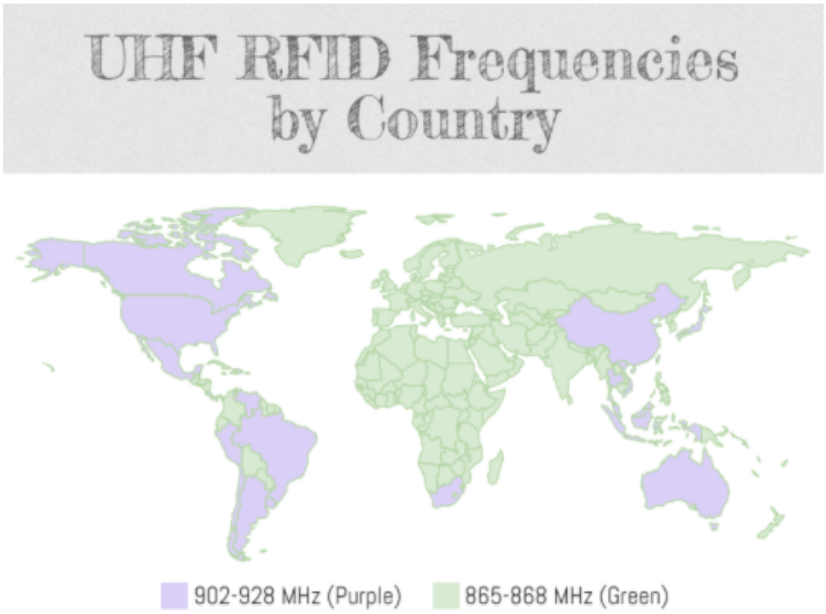

Figure 2.6: UHF Frequencies worldwide. (extracted from [11])

In the case of Portugal, the regulator Autoridade Nacional de Comunicações (ANACOM) stipulates that the band to be used is 865-868 MHz, and therefore the RFID tags designed in this thesis are to operate in this frequency band.

Most RFID tags and barcodes that contain an EPC are governed by standards and guidelines created by EPCglobal [13]. This EPC is the responsible component to create an unique identification for each tag. In the figure 2.7 below presents the EPC structure.

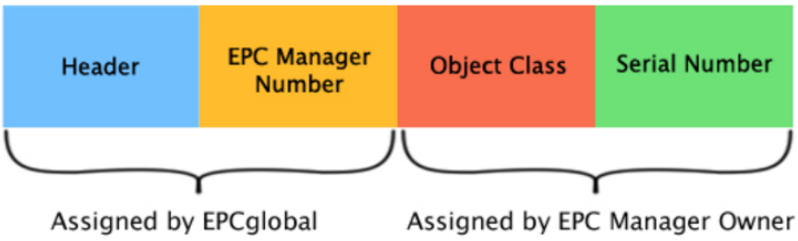

Figure 2.7: EPC structure. (extracted from [6])

It's composed by four elements: the header, EPC manage number, object class and serial number. The header identifies the length, type, structure, version and generation of the EPC. Th EPC manager number is the entity responsible for maintaining the subsequent partitions. The object class identifies a class of product. The serial number is a unique identifier number for each product. EPCs are encoded on RFID tags and are

designed to be uniquely among all -RFID tags and all categories of objects using tags in the world.

2.5 RFID technology state of the art

The RFID technology is a data collection technology whose goal is to automate the process of collecting or providing data about a product with which it is associated. This technology can be compared with technologies with similar objectives such as the barcode. Both technologies are very present in the retail market. In the table 2.2 comparisons between RFID and barcode technologies can be analysed.

Table 2.2: RFID and barcode comparison. (adapted from [14])

Attribute	**Barcode**	**RFID**
Line of sight	Required	Not required (in most of the cases)
Read ranges	Several centimeters to three decimeters	Passive RFID up to ~10 m Active RFID up to ~30 m
Technology used	Optical (laser)	Radio Frequency
Read/Write	Only read	Read and write
Automation	Most barcode scanners need humans to operate	Fixed scanners (readers) do not need human labor
Reliability	Wrinkled and smeared tags do not work	Nearly flawless read rate
Data Capacity	<20 characters	100 to 1000 characters

One of the biggest differences is the need for line of sight. Barcoding uses optical laser technology, where there is an absolute need for the scanner and the barcode to be in line of sight or else reading is not possible. As the technology used in RFID is radio frequency, the signal can pass through objects, so there is no need for the reader to be in line of sight with the tag. However, the fact that there is no line of sight may in some cases mean a lower power transfer due to signal losses when penetrating objects, which may lead to a shorter reading distance. Even so, the reading distance of a RFID system is far greater than that of a barcode system. Another advantage is the possibility of reusing the tags, being able to change the data present in the tag and, with some conditions, apply it to another product. Re-use is not possible in the barcode. Finally, the RFID technology is completely automatic, meaining that no human action

is required for operation after installation while the barcode scanner, in the majority of the cases, is handheld.

Despite the advantages that RFID technology brings to the retail market when compared to the currently existing legacy barcode technology, there are some great drawbacks that hinder its massification.

One of the most experienced difficulties is the cost of implementing readers and tags. Although the price of the tags is much lower than the price of the readers, their total price becomes significantly higher. Imagining the implementation of a RFID system in a retail supply chain with a large scale, one realizes that there is a great need for constant tag replenishment in the processed products, unlike readers that require little maintenance [15]. Hence the cost of tags becomes much higher than the cost of readers, and the cost of a RFID system becomes much more expensive than the current barcode.

Another difficulty is the effect that the different materials of the products have on the antenna power pattern. A RFID tag may work perfectly well when applied to a package of cookies, but the same tag is unlikely to work when applied to a bottle with liquid in it, or to some product that contains a metal package. This is due to different RF behaviour that occur on these materials. The liquid on the bottle will refract a large portion of the wave, and the metal package will reflect it [16]. This implies that each tag has to be designed according to the product to which it will be applied on. Besides this factor, there is also a lack of consistent UHF spectrum allocation worldwide, with different operating frequencies for RFID depending on the country or continent. This means that the tag must either be designed according to the operation frequency established on the country for which the product will get distributed, meaning that different tags are needed for the same product, or the tag as to be designed covering the whole RFID frequency spectrum to be able to work worldwide.

Given these disadvantages of the technology, there is still a need to study and solve issues related to the design of cost-effective RFID tag antennas for the identification of objects that have irregular surfaces and with materials adverse to radio frequency functionality [17]. It is particularly challenging to create an antenna that performs well when applied on a liquid filled-bottle due to the high conductivity, permittivity and variety of the liquid [18]. The cylindrical shape of a bottle makes the radiated field of the current also depend on the radius of the cylinder, thus on the radius of the bottle [17]. So, these aspects are necessary to take into account when designing a tag antenna to work on objects of this nature.

The literature [18] presents a simple antenna structure of a folded dipole that works when applied to a plastic bottle filled with water. This antenna is 8 cm long and 2.4 cm wide. Results of 8 m reading distance are achieved with the antenna in free space

and 4.2 m with the antenna applied to the bottle filled with water, for the frequency of 915 MHz. Next, improvements are made to the antenna to enhance its performance. In order to improve its gain, the dipole arms are changed into a zig-zag or meandered shape. With this the arms are no longer parallel, not causing currents to flow in opposite directions and mutually canceling out their contributions to the far field radiation. The gain went from -10.8 dB to -5.54 dB. With the improvements made the total size of the antenna has decreased, having now 4.4 cm long and 2 cm wide. The reading distance has also increased with the tag now being read from 5.6 m away when applied to the plastic bottle filled with water.

In [19] an embedded T-match dipole UHF tag antenna mounted on a winebottle neck with a 360-degree readable zone is shown. Being mounted on the bottleneck causes the radio waves to pass through a smaller amount of wine, reducing or mitigating the loss introduced by the wine. The T-match dipole is chosen because of its adaptive impedance and wideband capability. It is also used an end loading technique to decrease the antenna size and a loading bar to ease impedance adjustments. This antenna yields read distance results between 5 to 8 m when the bottle is in an upstanding normal position, and 3 to 7 m when the bottle is upside down, having wine filling the bottleneck area. Both of these results are valid for a frequency range between 860 and 960 MHz, covering all the UHF RFID bands.

In [20] a flexible UHF RFID antenna applicable in most glass bottles with different liquids is presented. The antenna is formed by a rectangular strip folded into a low profile loop antenna. It is composed of four identical open-ended meandered lines for impedance tuning and it is matched around 925 MHz. Silicone rubber is used as the substrate, with 3 mm thickness and a permittivity of 2.8, which makes the antenna malleable. It has a total size of 7 cm in length and 3 cm in width. Although the tag has shown good power reflection coefficient values when applied both on the bottle body and on the bottleneck, it is chosen to apply the tag on the bottleneck since there is less influence of liquid from the bottle itself and from adjacent bottles, turning the tag orientation indifferent to horizontal plane thus increasing its identification probability and not covering bottles' existing label. Tests are made for different liquids including wine, vinegar and oil, with the tag antenna achieving reading distances between 1.5 and 2 m. This tag presents advantages such as low profile, easy installation and robust performance across different liquid types.

The literature [21] demonstrates an antenna tag applicable in a new type of wine bottle closure. This closure is composed of a thin metal sheet, a hollow internal plastic bladder and a plastic cover. The space in the internal bladder is used to place the RFID tag antenna. The antenna is a meander line monopole matched for 920 MHz, 2.6 cm

long and 1.5 cm wide. A circular ground plane capable of fitting in the bottle closure is used to allow the antenna to radiate over the metal structure. Part of the monopole is bent over this ground plane in order to obtain low profile performance, creating an Inverted F Antenna (IFA). Reading distances of 1.5 m are achieved for this tag antenna when applied on the wine bottle closure.

In [22] a small loop-based module is used to excite two dipole antennas by inductive coupling. It is possible to apply this combined two dipole antenna in a plastic container, getting its identification if the container is with or without liquid inside, one of the dipoles resonates when the container is empty and the other when the container is full. The combined antenna has a total length of approximately 5 cm and a total width of 4 cm and is designed to resonate at a frequency of 868 MHz. When applied to an empty plastic container, this antenna achieves read distance values of 3.7 m. However, this distance drops to 31 cm when the container is filled with water.

The described literature introduces different antenna designs adapted for different bottles, different liquids and different tag mounting positions. However, it can be concluded that the tag antenna is deeply influenced by the liquid present in the bottle due to the degradation it causes to the overall tag efficiency. It is clear that it is difficult to develop a tag antenna that fits all combinations of bottles and liquids, being necessary to adjust the characteristics of the antenna to achieve the project goals.

3

Free space RFID tag antennas

This chapter describes the study of size reduction and impedance matching techniques as well as the design of a first antenna that is adapted to an RFID microchip. A meandered dipole from [23] is first replicated, for which a study is made of how its dimensions influence its impedance. Afterwards, this dipole is adjusted so that its size is reduced and fits the outlined dimensions, ensuring that it is still adapted to the microchip, in a free space environment. Finally, a real situation is simulated, where the antenna is bent and placed on a hollow glass block to study the effect that this material has on the antenna's performance, just as if the antenna was applied to a bottle. A block of water is also placed on the hollow part of the glass cylinder to draw conclusions from the combined influence of these two materials.

3.1 Impedance matching and size reduction techniques

One of the most important factors in passive RFID tags is the reading distance. In order to obtain a good reading range, it is necessary to have the maximum possible power transfer between the antenna and the microchip. For this purpose, the impedance value of the antenna has to be as close as possible to the conjugated impedance value of the Integrated Circuit (IC). If these are exactly the same then maximum power transfer is obtained. The vast majority of RFID microchips in the UHF band have a capacitive impedance roughly ranging from -100 Ω to -400 Ω, being the real part an order of magnitude below. That said, the antenna impedance must be inductive in order to obtain conjugate matching [24].

Dipole antennas are widely used in RFID technology due to their simple structure and high efficiency [25]. Furthermore, dipoles are easily tunable antennas which allows to adjust their dimensions in order to make them more compact and at the same time achieve impedance matching with the IC. To achieve this match, parametric antenna study and optimization is performed until the requirements of the design or application for which the tag will be applied are performed in simulation. It is also important to notice that since the goal is to apply it on a bottle, its dimensions and size are relevant as the tag should not be oversized. Tag antennas are usually analyzed using electromagnetic modeling and simulation tools because their analytical analysis tends to be complex [26]. In this dissertation the CST Studio Suite [27] is used to perform all simulations and analysis of the antenna characteristics.

Taking this into account, techniques for impedance matching and antenna size reduction are now studied.

3.1.1 Planar dipole with T-Match

One way to change the impedance of a dipole is with the introduction of a centered-short-circuit stub. This technique is called T-Match. This centered-short-circuit stub can be interpreted as a second dipole, smaller than the main dipole, whose arm ends are shorted to the main dipole [24] [28]. The application of this technique to a planar dipole can be seen in the figure 3.1. This was the example chosen for this study since a conventional cylindrical dipole is not feasible to implement in a bottle due to its shape and the volume it occupies.

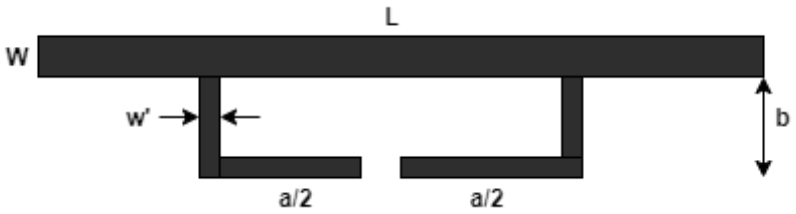

Figure 3.1: T-match of a planar dipole. (adapted from [24])

As can be seen in the figure 3.1 the second dipole of length a is placed at a distance b from the main dipole whose length is L. By changing the values of a, b, w and w', the input impedance of this antenna changes and can be adjusted to the impedance of the microchip.

In order to better understand how these dimensions influence the impedance, this antenna is studied with simulation. The main dipole is a half-wave dipole because, as

referenced in the literature [24], the resulting impedance in a dipole of this type is inductive. The length of this dipole is calculated for 866 MHz, and its length is obtained with the equation 3.1 where L represents dipole's length and λ the wavelength.

$$L = \frac{\lambda}{2} = 17,3cm \tag{3.1}$$

The T-Match can be seen in figure 3.2 where a = 20 cm, b = 4cm, w = 3cm and $w' = w/3$. These values are chosen taken into account the T-Match matching chart in [24].

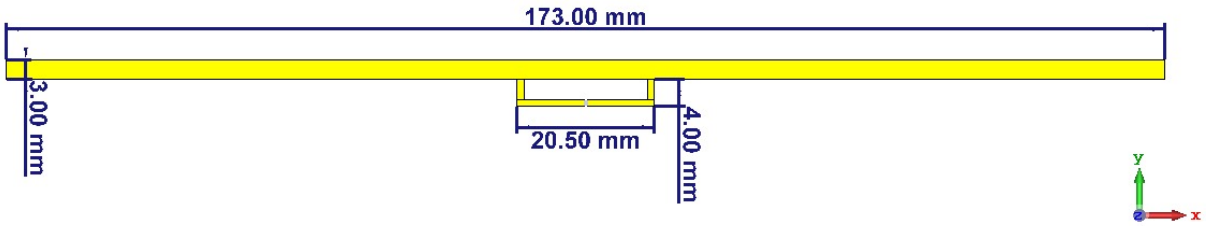

Figure 3.2: T-match antenna designed.

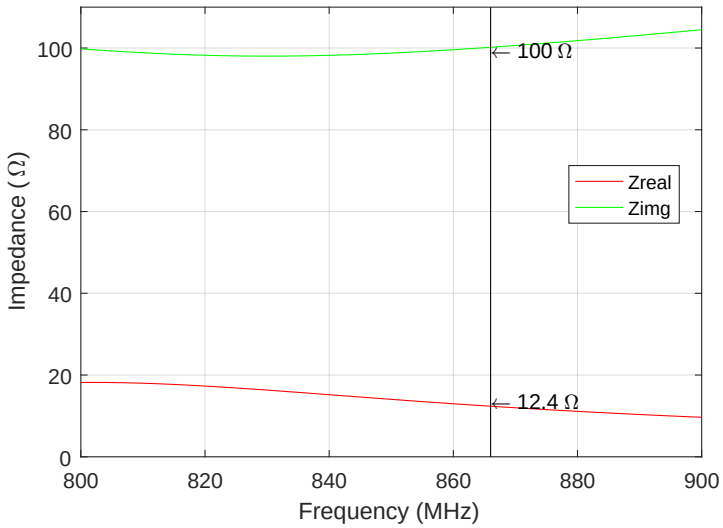

Figure 3.3: T-match antenna's impedance.

The length a of the second dipole has an addition of 0.5 mm to account for the space needed to place the microchip. Simulating this antenna an impedance value of 12.4 + j100 Ω is obtained at 866 MHz, as shown in figure 3.3. Having obtained the antenna's impedance, tests are now carried out with variations in the antenna's dimensions to evaluate how they change its impedance.

Table 3.1: Variation of T-Match antenna's dimensions and corresponding impedance value.

Dimension	Values	Impedance value @866 MHz
2*a	15 mm	6.6 + j77.3 Ω
	25 mm	20.3 + j122.5 Ω
2*b	2 cm	4.4 + j59.7 Ω
	6 mm	18.5 + j126 Ω
2*w	2 mm	17.8 + j108.7 Ω
	4 mm	9 + j89.6 Ω

Table 3.1 shows the impedance values obtained by varying the antenna dimensions. As can be seen, when an increase is made in the length of the second dipole the impedance value, both the real and imaginary parts, increase. The same happens with the distance b between the two dipoles. However when increasing w, and thus also increasing w', there is a decrease in the impedance of the antenna.

3.1.2 Inductively coupled loop

Similar to T-match, the inductively loop technique is also widely used for UHF RFID tags. In this technique a loop is placed at a small distance from the dipole as shown in figure 3.4. The strength of this coupling is controlled mainly by the distance between the loop and the dipole and the shape of the loop [29].

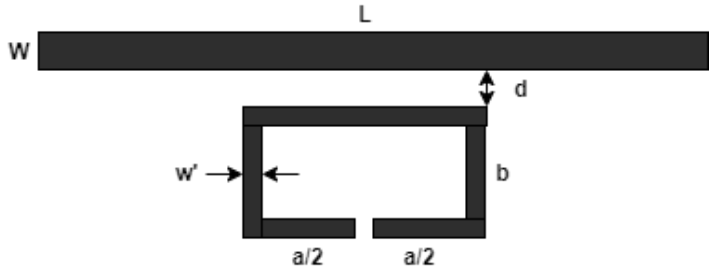

Figure 3.4: Inductively coupled loop technique. (adapted from [24])

Unlike T-match, there is no second short-circuited dipole, but instead a rectangular or square loop at a distance d from the main dipole. By varying its geometric dimensions a and b it is possible to adjust the size and shape of the loop, thus changing the total impedance of the radiating body [24] [29].

To test the influence of these dimensions on the impedance, this antenna is studied with simulation. A half-wave dipole is also considered, with length $L = 17.3$ cm in

order to make comparisons between both techniques fair. The antenna designed in the software can be seen in figure 3.5.

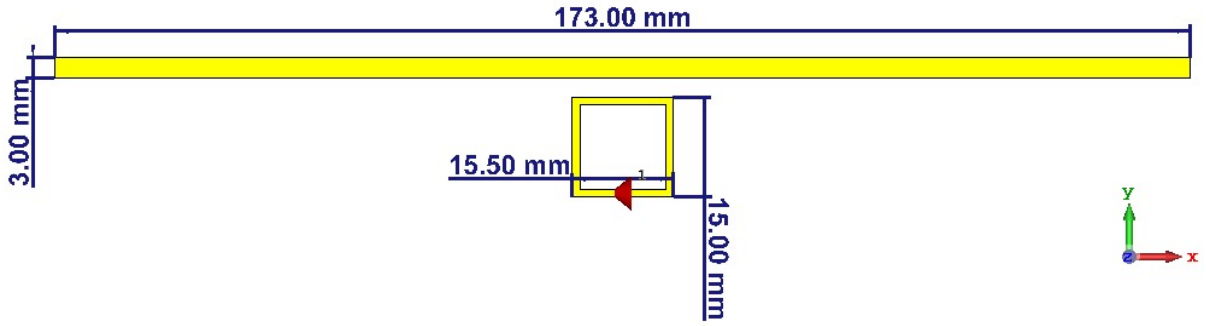

Figure 3.5: Inductively coupled loop antenna designed.

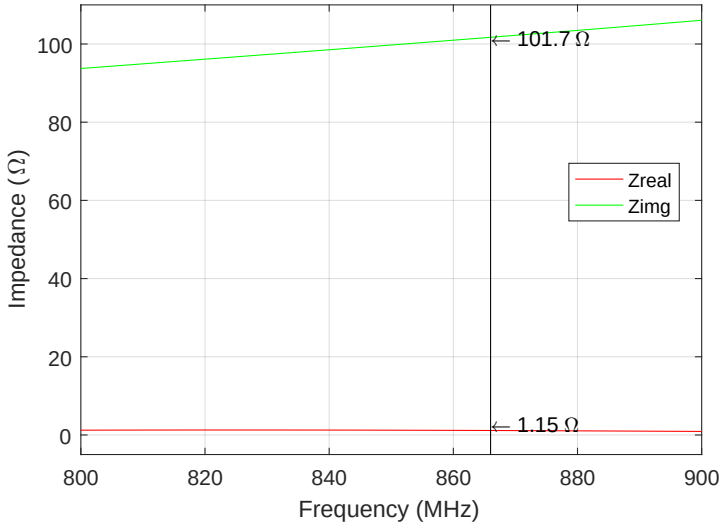

Figure 3.6: Inductively coupled loop antenna's impedance.

The loop is initially created with both dimensions a and b having 1.5 cm. Again, the extra 0,5 mm that the a dimension displays is taking into account the space needed for the microchip. The thickness of the dipole w has a value of 3 mm and the thickness of the loop is $w' = w/3$. The initial spacing between the dipole and the loop is 3 mm. For these dimensions, this antenna has an impedance value of 1,15 + j101.7 Ω at 866 MHz, as shown in figure 3.6. When compared to the impedance of the T-match antenna, it can be concluded that it has a much lower real part and a very similar imaginary part.

Simulations are now performed with dimensions of the antenna to evaluate their influence on the impedance. By analyzing table 3.2 it is clearly noticeable that the shape of the loop has a great influence, both in the real and imaginary part.

Table 3.2: Variation of inductively coupled loop antenna's dimensions and corresponding impedance value.

Parameter	Values	Impedance value @866 MHz
2*a	5 mm	0.27 + j57.33 Ω
	15 mm	2.87 + j144.63 Ω
2*b	5 cm	0.39 + j56.98 Ω
	15 mm	2 + j145.97 Ω
2*d	2 mm	1.5 + j101.44 Ω
	4 mm	0.94 + j101.71 Ω

By varying the dimensions a and b there is a direct variation on the value of the total impedance of the antenna. That is, by decreasing these dimensions the impedance value decreases, and vice versa. As for varying the distance between the dipole and the loop, d, it is noticeable that this has a greater influence on the real part and little influence on the imaginary part.

3.1.3 Meandering

Although the two techniques studied are usefull to adjust the antenna impedance to the IC impedance, antenna size may still be an issue. Considering that the half-wave dipole is the most used type of antenna for UHF RFID [**?**], it would had to have a length of approximately $17cm$ to work at a frequency of 866 MHz, as showed earlier. An antenna of this length is o long to be applied to a bottle. Therefore, there is a need to study size reduction techniques in order to be able to reproduce antennas with similar impedance values but with much shorter lengths/areas.

A popular technique used in printed dipoles size reduction is called Meandering and it consists in zig-zagging the straight horizontal segments of the half-wave dipole. The meandering effect can be observed in figure 3.7.

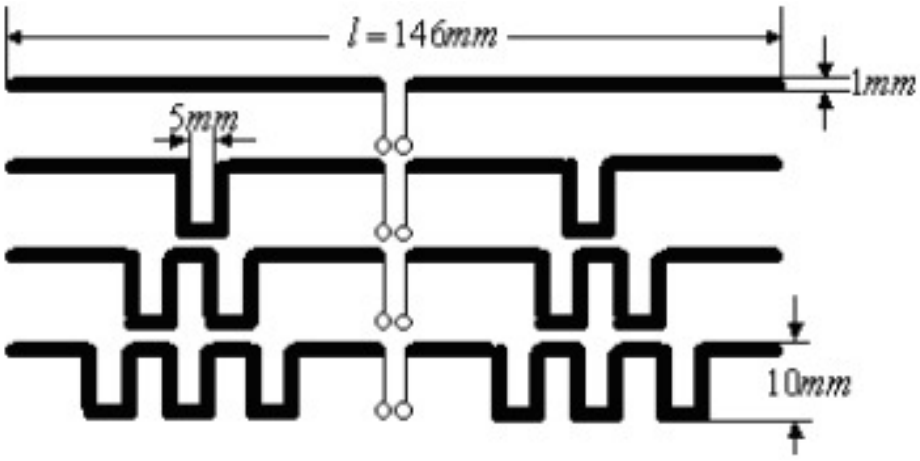

Figure 3.7: Meandering dipole scheme. (adapted from [25])

In this example the horizontal length of the dipole remains the same and meander sections are added to increase the total length of the conductive metal surface area. With the increase in the number of meander sections, and assuming that the other geometric parameters of the antenna remain constant, the resonant frequency of the antenna moves to lower frequencies [25] [**?**]. However there is a consequence to bending the arms of the dipole. Since current starts flowing in opposite directions, they cancel each other out, resulting in a reduction of antenna efficiency and gain [**?**].

In the figure 3.8 three antennas can be seen: the conventional half-wave dipole already used in previous simulations and two other versions of this dipole, one with one meander section and the other with two meander sections.

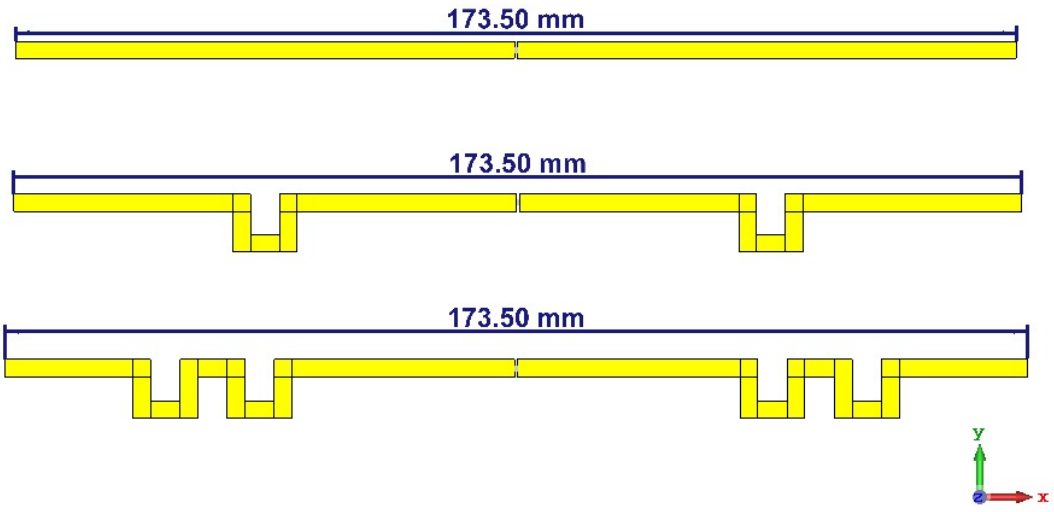

Figure 3.8: Designed meandered dipoles

The S_{11} values of these antennas can be seen in figure 3.9. As can be concluded, it proves that the resonance frequency is shifted to lower values the greater the number of meander sections.

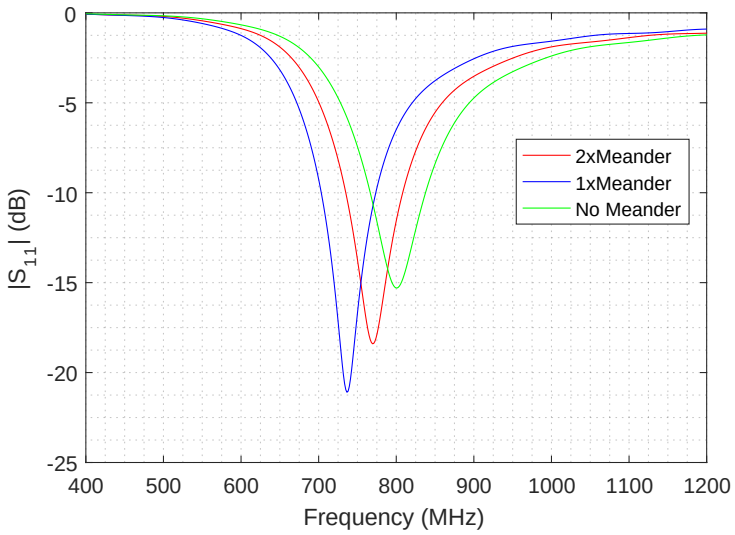

Figure 3.9: S_{11} value of designed meandered dipoles

By applying this technique it is possible to retune the antenna to other frequencies in order to match it to the desired one.

3.1.4 Tip loading

Another size reduction technique for antennas of this type is the Tip-Loading [25]. This technique consists of increasing the conductive surface at the end of the dipole, as show in figure 3.10. This increases the number of charges that accumulate at the end of the antenna, and consequently its capacitance [25] [**?**]. With this capacitance increase, the resonant frequency of the antenna lowers, since it is inversely proportional to the capacitance [**?**]. In figure 3.10 the structure of the tip-loading technique can be seen.

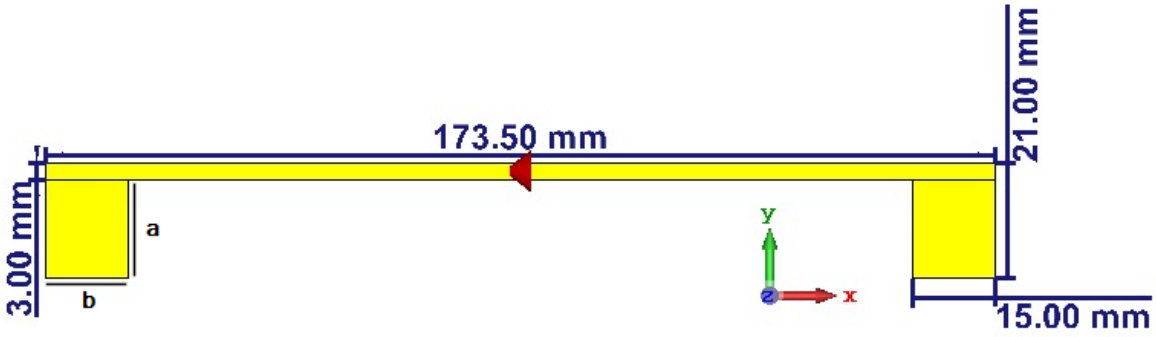

Figure 3.10: Tip Loading technique.

By changing the value of a and b the end of the dipole tips is changed. A graph of the results is shown in the figure 3.11. It is possible to observe the changes caused in the resonant frequency due to the variation of the tip loading.

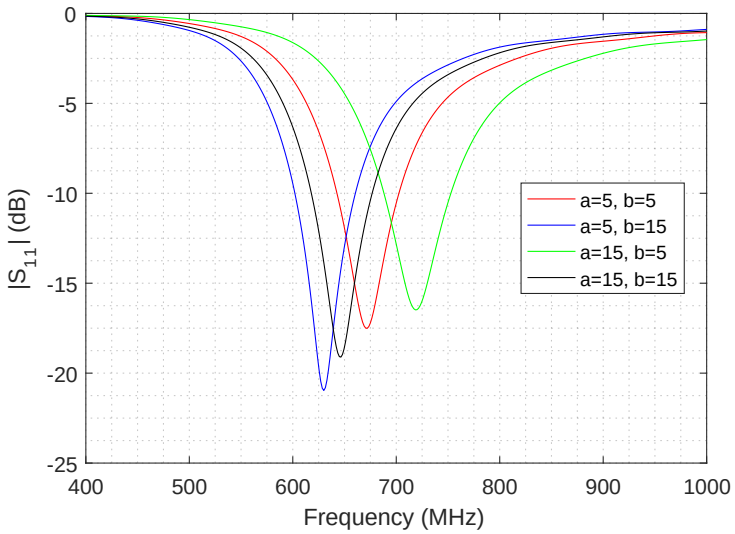

Figure 3.11: S_{11} value with varying values for a and b.

By increasing the geometrical variables a and b the capacitance of the antenna increases, which causes a decrease in the frequency. Therefore, in order to bring this frequency back to UHF RFID band values it is necessary to reduce the total size of the antenna.

3.2 Meander dipole

A tag antenna that already employs both the meandering technique for size reduction and T-match for input impedance matching previously discussed is presented in [23]. The tag antenna presented in [23] was designed to operate in free space and will be used as a basis for the present work.

The tag was designed to work in the UHF RFID band and in a free space environment, without any restriction in terms of dimensions, using the Murata LXMS31ACNA-010 microchip with an input impedance of 12 - j107 Ω at 866 MHz [30]. The tag is shown in figure 3.12 with dimensions shown in table 3.3.

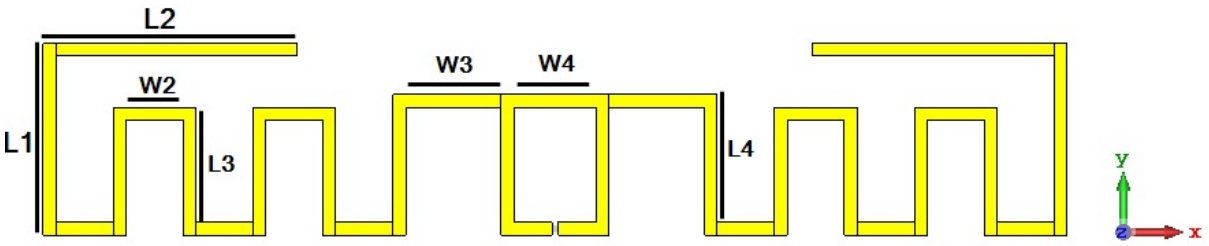

Figure 3.12: Replicated meandered dipole.

To achieve conjugate impedance, since the impedance of the IC used with this antenna has a value of 12 - j112 Ω, at 866 MHz, the ideal value for the impedance of the antenna would be 12 + j112 Ω.

After the antenna is designed in the software and the discrete port defined , it is now possible to obtain the antenna impedance through simulation. The real and imaginary part of the antenna impedance can be observed in the figure 3.13. The impedance value is 12.4 + j117.2 Ω at 866 MHz, which is close to the IC impedance value.

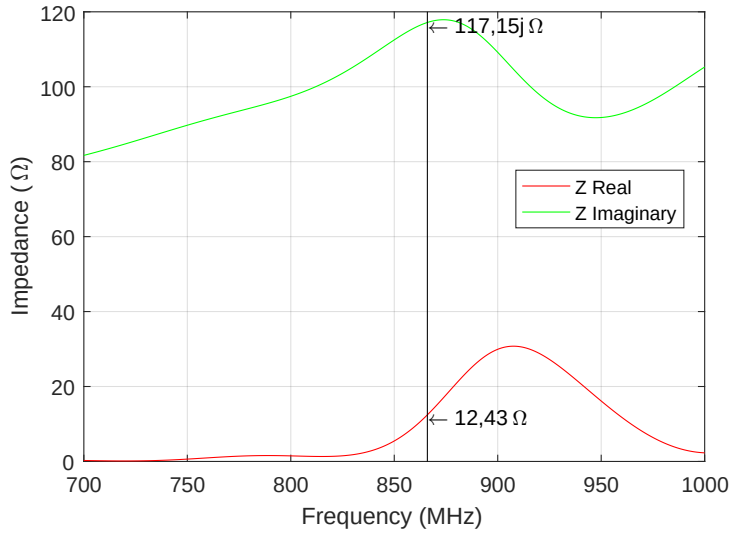

Figure 3.13: Meandered dipole impedance.

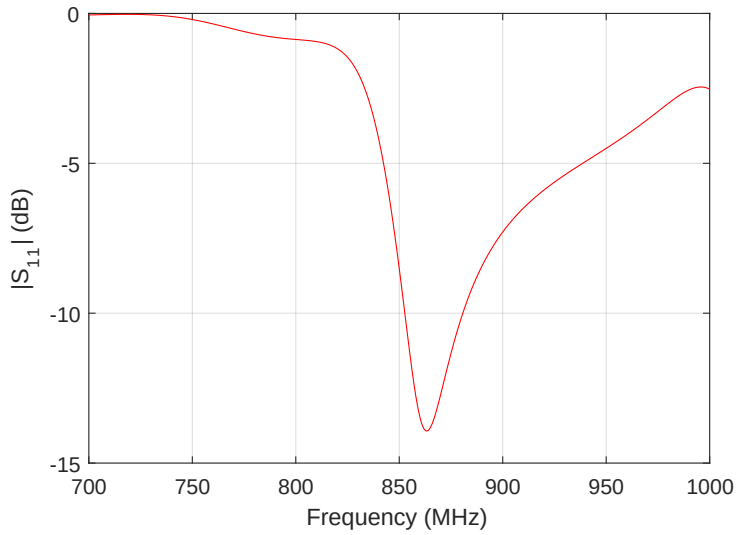

Figure 3.14: Meandered dipole S_{11} parameter.

The S_{11} parameter of the replicated meandered dipole can be seen in the figure 3.14. A feeding port of 12.4 - j 117.2 was used. It has a minimum value of -13.93 dB at a frequency of 863 MHz and at the frequency of 866 MHz it has a value of -13.67 dB. Since this parameter has a value below -10 dB it can be concluded that this antenna is well adapted to the microchip.

The dimensions of the antenna are a critical factor to take into account when applying it to a bottle. Although there are bottles with labels of various shapes and sizes, it was

decided that the antennas to be developed should not be more than 3 cm high and 6 cm long, in order to be able to mount the tag behind the bottle label so that it is not so visible.

Since the replicated antenna, present in table 3.3, has a total dimension of 1.5 cm high and 8.05 cm long, it is necessary to reduce its size to fit the designated parameters while still making sure that it is adapted to the tag chip.

Table 3.3: Meandered dipole antenna dimensions.

Parameter	**Dimensions [mm]**
L1, L2, L3, L4	15, 20, 9, 10
W1, W2, W3, W4	1, 4.5, 8.5, 6.5
g	0.5

In order to understand how the dimensions of the tag could be modified to achieve a compact tag with the maximum allowed size, a parametric study of the antenna is executed. The effect of L1, L2, L3, L4, W1, W2, W3, W4 on the input impedance is shown in figures 3.15 to 3.30, respectively.

In the figures 3.15 and 3.16 are represented the real and the imaginary part of the impedance deviation caused by the variation of 1*mm* in the L1 measurement.

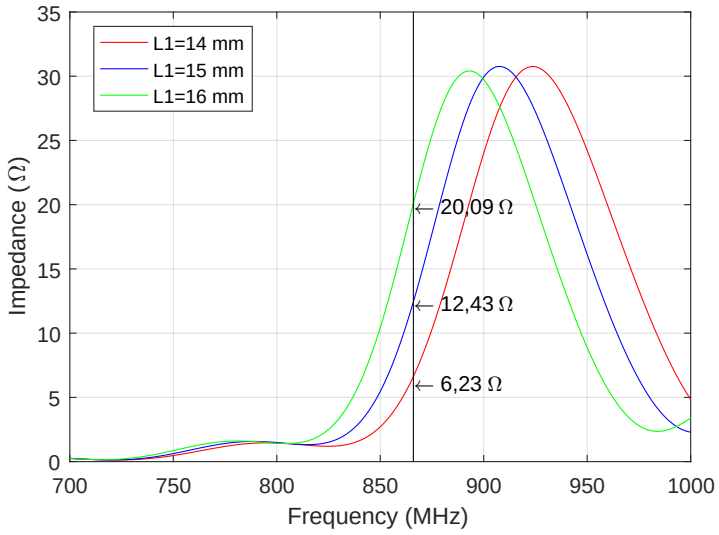

Figure 3.15: Impedance's real part as a function of L1.

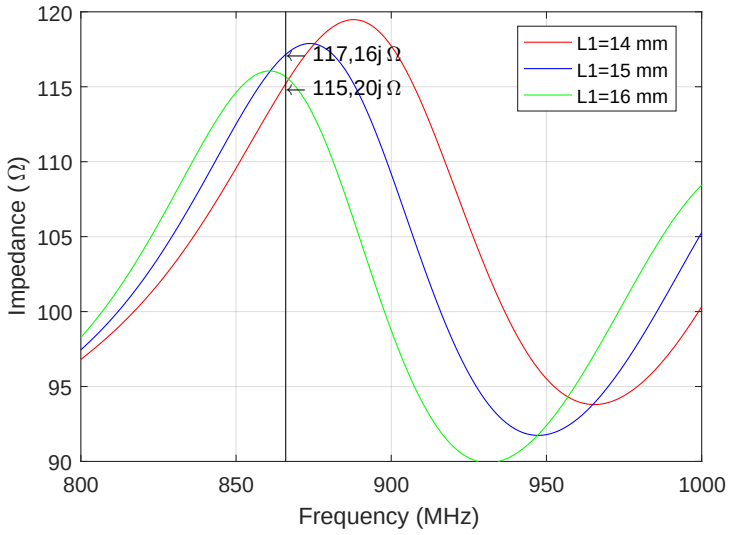

Figure 3.16: Impedance's imaginary part as a function of L1.

When analyzing the simulation results it can be concluded that the real part of the impedance varies directly with the dimension L1. That is, when L1 is decreased, the real part of the impedance is also decreased and if this measure is increased the impedance is also increased. However, it is not linear. On the other hand, the imaginary part of the impedance always decreases regardless of whether L1 is increased or decreased. It can be deduced that the variation of L1 has a greater impact on the real part than on the imaginary part since with the same variation of 1 mm a greater difference in the real impedance was obtained. Considering these orders of magnitude, this measure can be used to make a greater adjustment in the real part without seriously changing the imaginary part of the impedance.

Regarding L2, on figure 3.17 we can conclude that the variation in L2 causes a direct change in the real part of the impedance, just like what happened with L1. When increasing this length the real impedance increases and when decreasing it, the real impedance also decreases. The magnitude of these deviations is around 3 Ω which is less than the magnitude of the changes caused by the L1 measurement. By changing the value of this measurement it is possible to make a finer adjustment to the impedance value that with L1. As for the imaginary part, it is concluded that it suffers smaller changes when compared to the variation caused by L1 dimension.

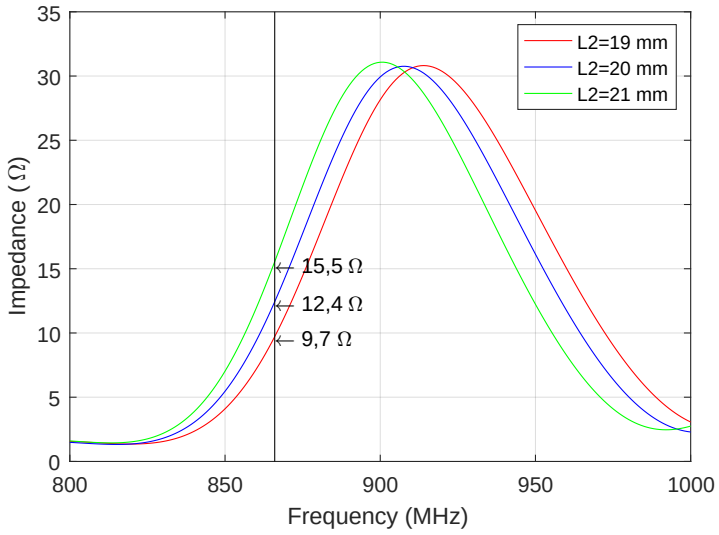

Figure 3.17: Impedance's real part as a function of L2.

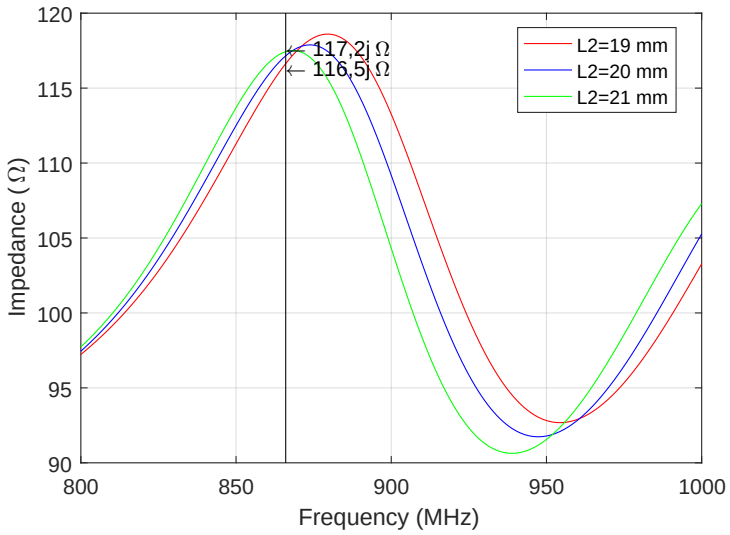

Figure 3.18: Impedance's imaginary part as a function of L2.

Therefore, by altering L2 a finer adjustment can be obtained in the real part than with L1, at the expense of a very small alteration in the imaginary part value.

The deviation caused in the impedance by the variation in the size of the parameter L3 can be seen in the figures 3.19 and 3.20.

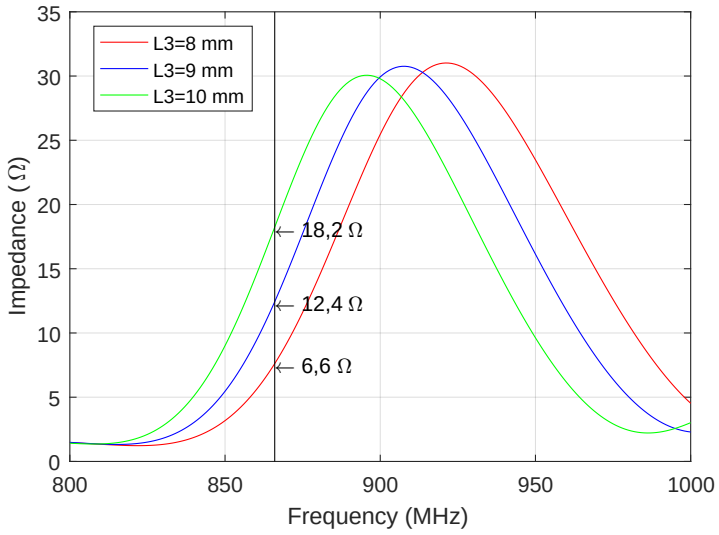

Figure 3.19: Impedance's real part as a function of L3.

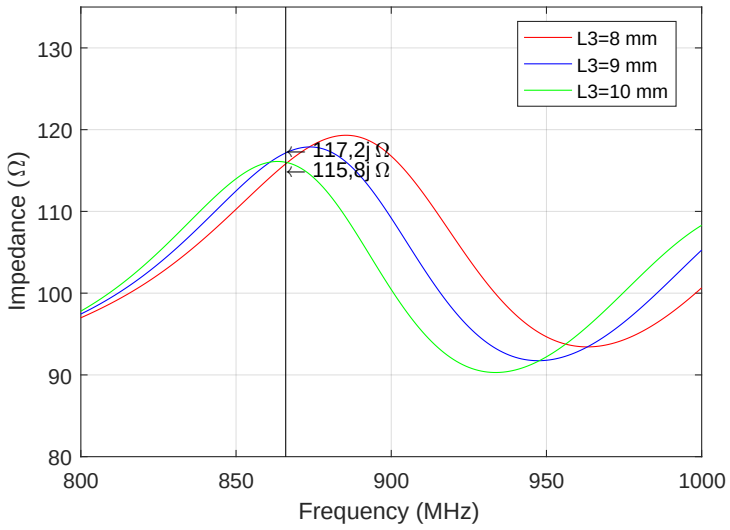

Figure 3.20: Impedance's imaginary part as a function of L3.

This parameter defines the height of the dipole arms. It should be noted that both the height of the central ring and of the first components of the arms connected to it are defined by parameter L4, which was kept constant in this simulation. Analyzing both figures we can conclude that the deviations are similar to the variations caused by L1 and L2 previously analyzed. The real part also evolves directly with this measure, presenting a deviation of 5 Ω when L3 decreases and 6 Ω when L3 increases. Concerning the imaginary part, independently of the increase or decrease of L3 the impedance decreases, such as seen with the L1 variation.

Based on the analysis of the effect of L1 and L3 it can be concluded that it is not the distance between the upper and lower arms of the dipole that has the impact on the real part of the impedance. Reason for this is that if L1 is increased, and consequently the distance between these two parts increases, the real impedance increases. On the other hand, if L3 is increased and the distance between these parts decreases, the impedance also increases.

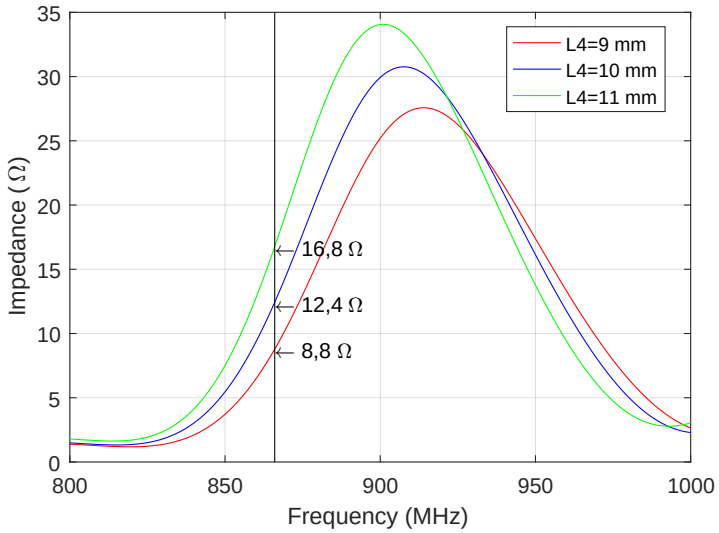

Figure 3.21: Impedance's real part as a function of L4.

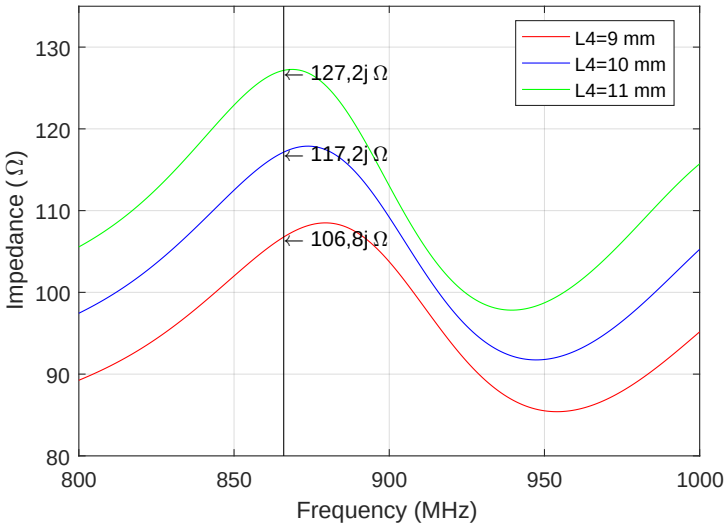

Figure 3.22: Impedance's imaginary part as a function of L4.

The change in the impedance caused by the variation of the L4 can be viewed in figures 3.21 and 3.22. This dimension is the height of the central ring and also a component of

the dipole's arms. The influence of L4 in the real part of the impedance does not differ much from those obtained previously. It varies directly with the increase or decrease of L4, having a deviation of 4 Ω. However, it is the first dimension that demonstrates to affect the imaginary part, as can be recognized in the figure 3.22. When expanding or reducing L4 by 1 mm, the impedance shows an increase or decrease in its value of approximately 10 Ω, respectively.

Although it also substantially affects the real part, it is possible to adjust this dimension in order to obtain the desired value of the imaginary part of the impedance. Taking into account the low impact caused by the other dimensions in this imaginary impedance, it is possible to first achieve an ideal measurement for L4, where the imaginary conjugate of the microchip's impedance is achieved, and then adjust the dimensions L1, L2 and L3 to match it's real part value.

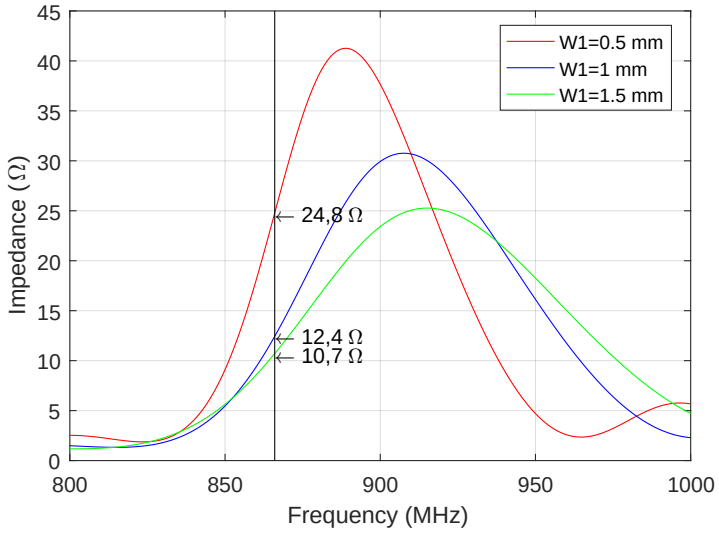

Figure 3.23: Impedance's real part as a function of W1.

Figures 3.23 and 3.24 show the impedance variation as function of W1. As can be deduced from both figures, when increasing W1, and thus increasing the antenna thickness, a decrease in both the real and the imaginary part is obtained. However, this variation in impedance is not linear. When decreasing 0.5 mm in W1, the real part shifts from 12 Ω to 24 Ω. However when the thickness is increased, the impedance only has a decrease of 2 Ω, approximately. The same can be verified in the imaginary part, although with different proportions. The positive variation has a value of 24 Ω, moving from 117 Ω to 141 Ω, while the negative variation has only a value of 14.5 Ω, reaching a value of 102.7 Ω when increasing W1.

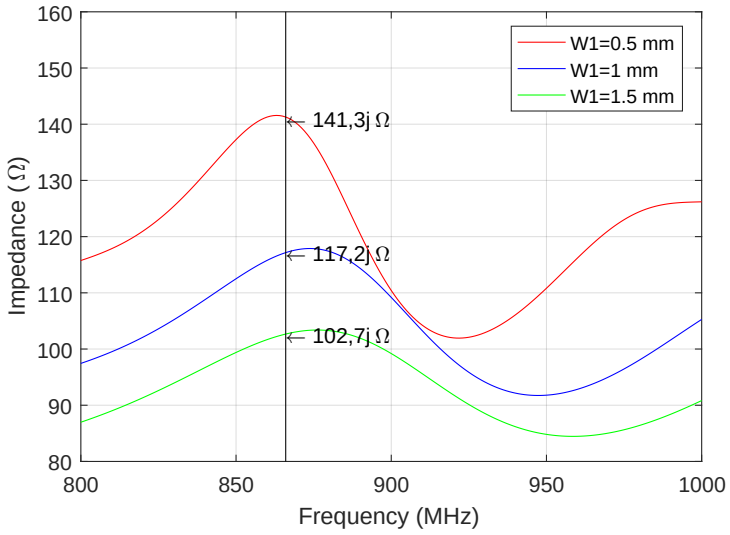

Figure 3.24: Impedance's imaginary part as a function of W1.

The variation of the impedance caused by the variation of the W2 dimension is represented in the figures 3.25 and 3.26. This dimension is the length of the arms of the dipole that are not connected to the central ring. It must be taken into account that a 1 mm variation in this measure causes a bigger increase in the total length of the antenna, since W2 is the length of four parts of the arms.

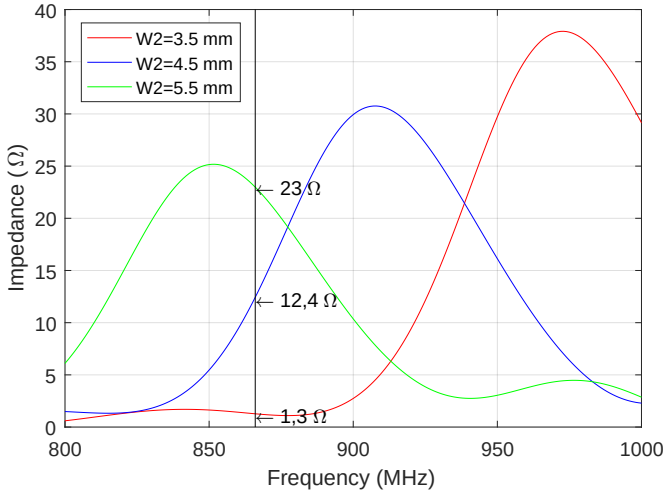

Figure 3.25: Impedance's real part as a function of W2.

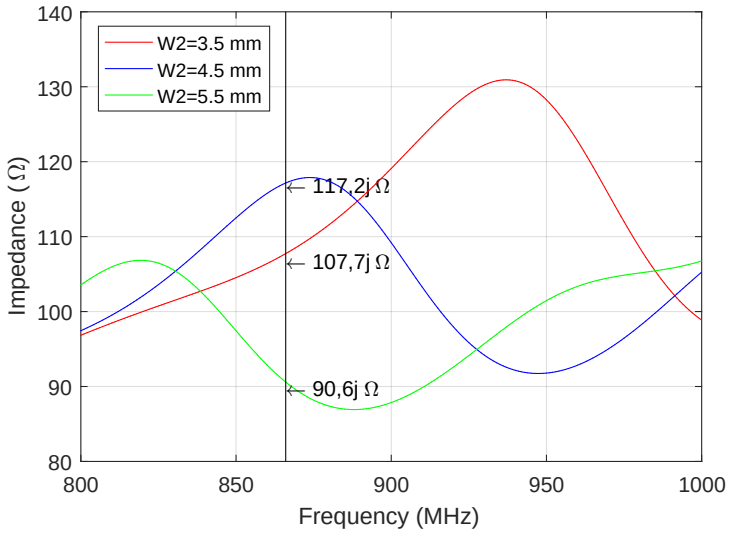

Figure 3.26: Impedance's imaginary part as a function of W2.

Considering figure 3.26, it can be seen that whether W2 is increased or decreased, the imaginary impedance decreases. If W2 is increased, the impedance shows a deviation of 27 Ω, going from 117 Ω to 90 Ω. If W2 is decreased, the deviation in the impedance is 10 Ω, changing to a value of 107 Ω.

The variation of the impedance with W3 can be seen in the figure. This measure represents the length of the initial part of the dipole arms.

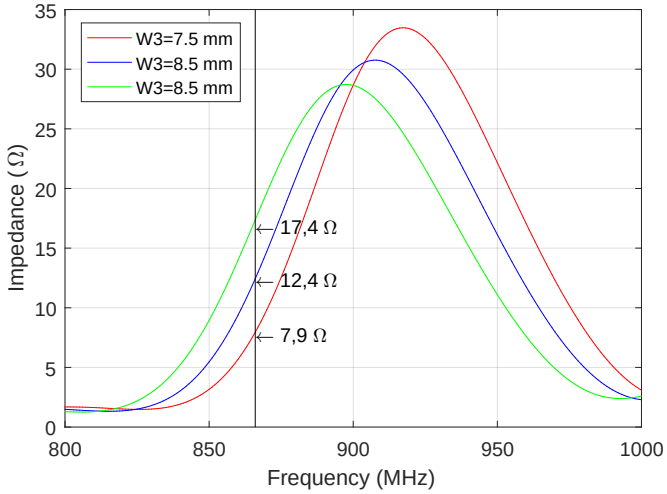

Figure 3.27: Impedance's real part as a function of W3.

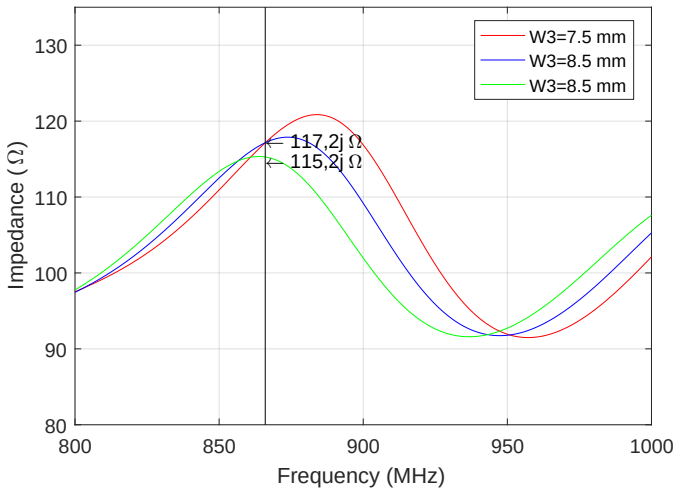

Figure 3.28: Impedance's imaginary part as a function of W3.

The real part of the impedance is the most affected with this dimension, as can be deduced by the figures. When increasing W3 by 1 mm there is a 5 Ω increase and in case of reduction of the size of W3 the real part decreases 4 Ω. Regarding the imaginary part, it remains practically unchanged with the variation of the length W3, decreasing only 2 Ω when increasing this measure.

The variation of the antenna's impedance caused by deviation in the W4 measurement can be observed in the figures 3.29 and 3.30. This measurement is the length of the center ring.

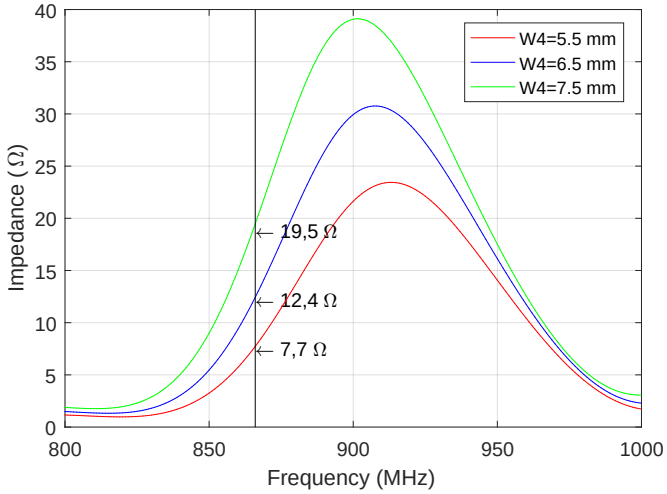

Figure 3.29: Impedance's real part as a function of W4.

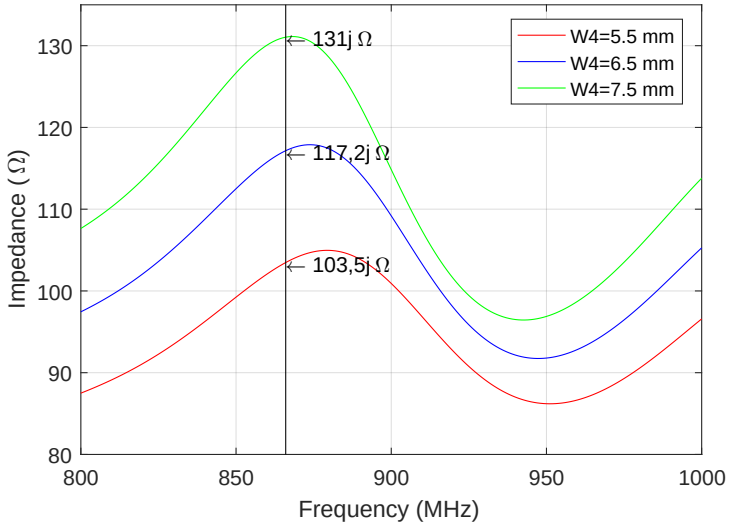

Figure 3.30: Impedance's imaginary part as a function of W4.

When analyzing the figures it can be concluded that the W4 variation causes considerable changes in both real and imaginary parts of the impedance. This is due to the fact that the dimensions of the center ring, the most influential component in the impedance of this antenna, are being changed. Paying attention to figure 3.29 and the real impedance's part, it can be seen that it presents a direct variation with the variation of W4, going from 12 Ω to 7.7 Ω when W4 decreases and to 19.5 Ω when it increases. The imaginary part of the impedance has a more substantial change. With 1 mm increase in W4, this impedance increases 14 Ω, from 117 Ω to 131 Ω, and with the decrease in W4 it decreases to 103.5 Ω.

3.2.1 Dielectric effect

In addition to testing all measures size change to see how they influence the impedance and consequently the adaptation of the antenna, it is also necessary to test the impact of the dielectric used. As the antenna will be manufactured using a inkjet-printing method [31], and therefore printed on paper, it makes sense to also study the influence of this material. A block of paper is placed bellow the antenna and a simulation of its impedance and S_{11} parameter is performed. This simulation is carried out with the original dimensions, so that the results can then be compared between the values of the original antenna and the antenna with the paper.

Figure 3.31 shows the antenna with the paper block underneath, in red.

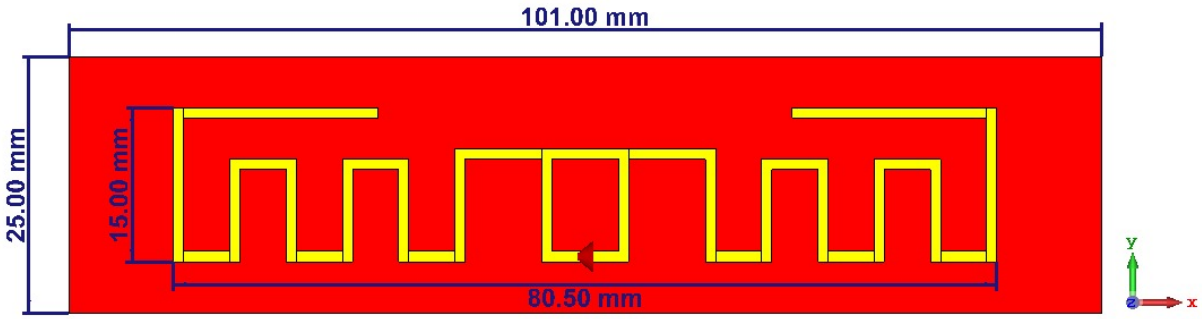

Figure 3.31: Replicated meandered dipole with block of paper.

This block of paper is created by adding 1 cm to each side of the antenna, and 0.5 cm to the top and bottom, with a total length of 10.1 cm and a total height of 2.5 cm. It is assumed that this is a conventional A4 sheet of printing paper and its thickness is 0.065 mm, as researched in [32]. The paper properties were obtained from CST library and presents a $\varepsilon_R = 2.31$ and $tan\delta = 0$. Figure 3.32 shows the impedance of the antenna with the paper block.

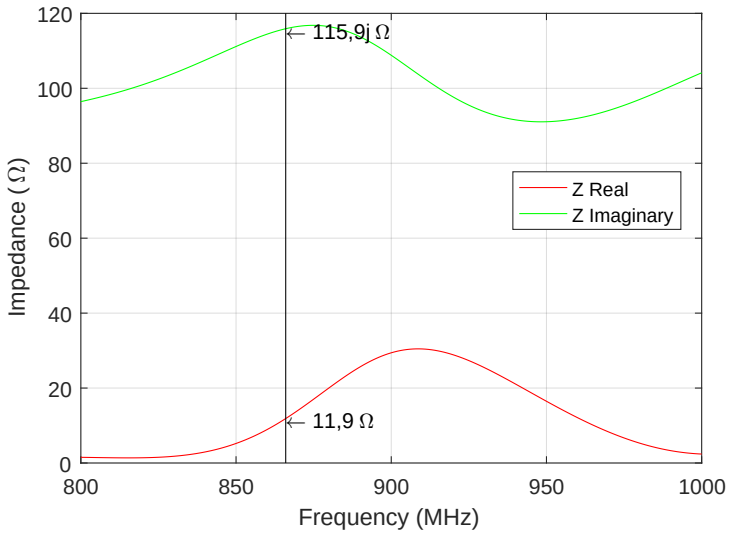

Figure 3.32: Replicated antenna's impedance with block of paper.

As can be seen, the antenna now shows an impedance of 11.9 + j115.9 Ω. When compared to the paperless antenna's impedance of 12.4 + j117.2 Ω we can conclude that the paper also affects the impedance slightly. The antenna parameter S_{11} with paper is shown in figure 3.33.

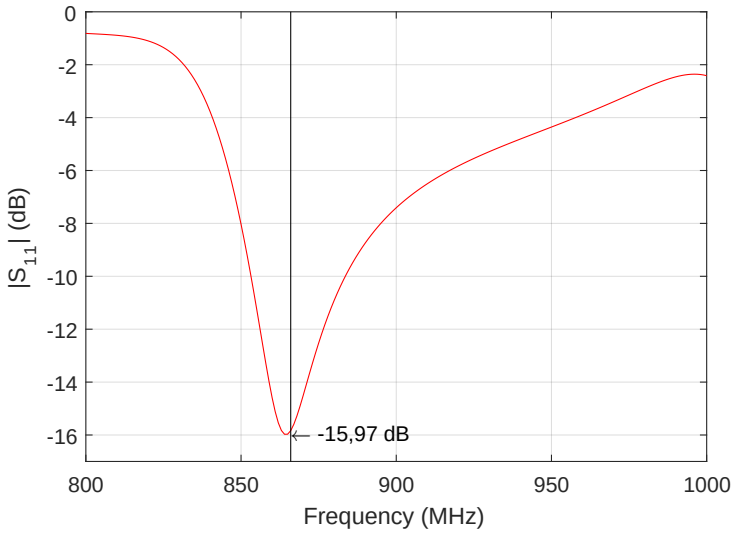

Figure 3.33: S_{11} parameter of replicated antenna with block of paper.

As expected after observing an approximation of the antenna impedance to the microchip impedance, there is an improvement in its adaptation. The antenna now has an S_{11} value of -15.8 dB, unlike the previous -13.7 dB, achieving an increase in adaptation of approximately -2 dB. Its bandwidth has hardly changed, being now between the frequencies of 853 to 883 MHz and having now a value of 30 MHz.

3.3 Compact meandered dipole

After the parametric study, the antenna is now modified to comply with the previously imposed maximum dimensions of 6cmx3cm and an impedance of 12 + j112 Ω at 866 MHz.

As the previous tag was to wide, the solution to obtain an even smaller tag is to lengthen the dipoles ends and create a top meander part, as shown in figure 3.34. The tag as a conductive part occupying 3 cm x 4.2 cm which extends to 4 cm x 6.2 cm if the paper substrate is taken in account.

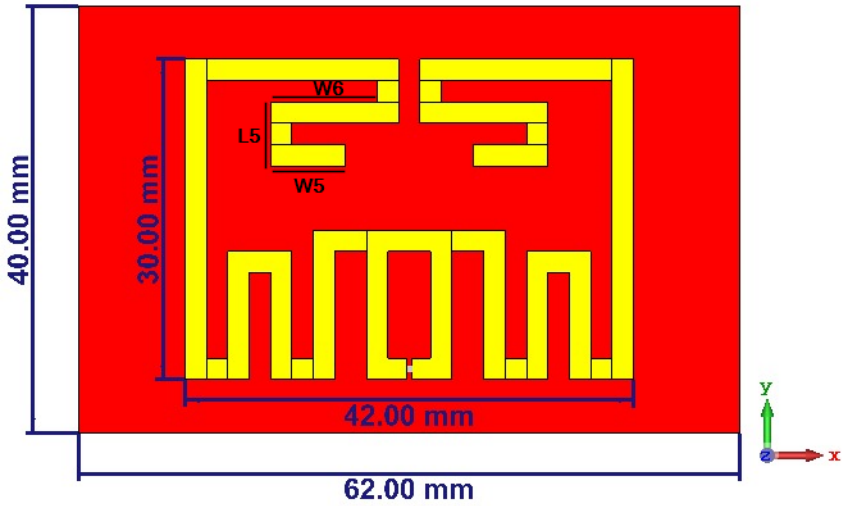

Figure 3.34: Meander dipole built from replica and adapted to microchip.

It can be noticed that it has a length of 4.2 cm, having achieved a reduction of 3.8 cm compared to the original one. Despite this reduction in length, it was necessary to balance the dipole by increasing its height in order to maintain its adaptation to the microchip. Its height has now doubled, having now a value of 3 cm compared to the previously 1.5 cm.

After manipulation of the several dimensions, the desired input impedance was obtained with the dimensions shown in table 3.4. The input impedance and S_{11} parameter are shown in figures 3.35 and 3.36 respectively.

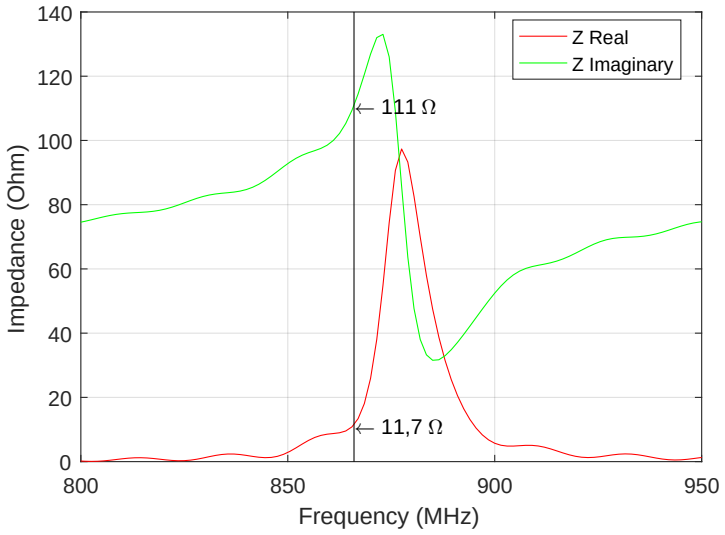

Figure 3.35: Built meander dipole impedance's imaginary part parameter.

It can be seen that the impedance of this antenna has a value of 11,7 + j111 Ω, very similar to the conjugated impedance of the microchip. However, both real and imaginary parts vary sharply as the frequency changes. The real part increases from 11.7 Ω to 13.5 Ω and the imaginary part from j111 Ω to 114.5 Ω with the increase of only 1 MHz in frequency.

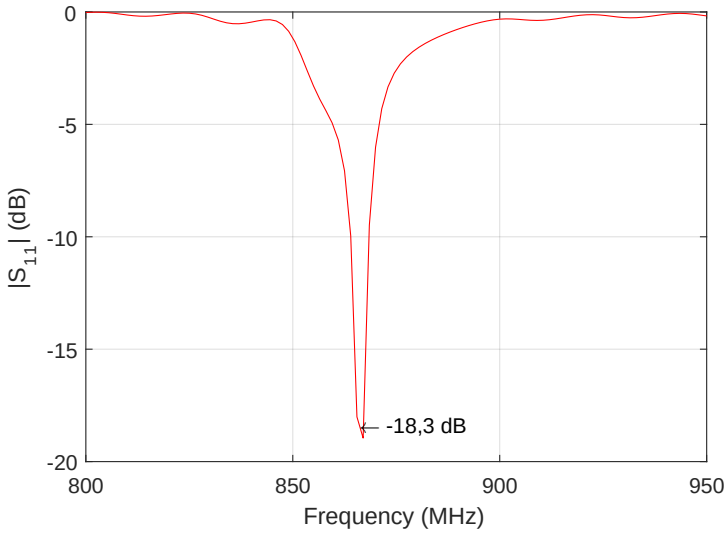

Figure 3.36: Built meander dipole S_{11} parameter.

The antenna is still well matched, having a value of -18.3 dB at a frequency of 866 MHz. The minimum value of this parameter is -19 dB at a frequency of 867 MHZ, but the difference between these is quite small. However, a large variation of this reflection coefficient with the frequency is also noticed, as a consequence of the abrupt variation of the input impedance. Therefore, the bandwidth of this antenna is much lower than the original, having now a value of 4 MHz, in the range from 854 to 868 MHz. Considering that the UHF RFID frequency band is only 3 MHz, between 865 and 868 MHz, it is not a bad factor that the antenna has a small bandwidth since it helps to eliminate noise from unwanted frequencies.

The antenna's input impedance is very sensitive to changes in its dimensions so it is needed to take in consideration that small manufacturing errors could completely unmatch the antenna to the desired frequency band.

Keeping in mind that the tag will be incorporated on a bottle, the effects that bending the antenna have on its behaviour are are now addessed. Typically glass bottles are 20 cm high, up to where the bottle neck starts, and about 10 cm from there until the end of it. They have a diameter of approximately 8 cm and a thickness of 2 mm [20].

Table 3.4: Adapted meandered dipole antenna dimensions.

Paramenter	Dimensions [mm]
L1, L2, L3, L4, L5	30, 20, 10, 12, 6
W1, W2, W3, W4, W5, W6	2, 2, 3, 4, 7, 10
g	0.5

The bent antenna is visible on figure 3.37. It is important to note that the dimensions of the antenna have not been changed and the radius of curvature is 4 cm.

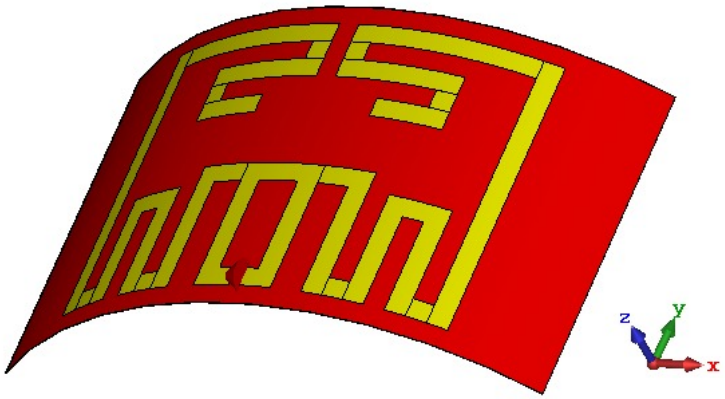

Figure 3.37: Bent built dipole.

The real and imaginary parts of the impedance can be observed in the figure 3.38.

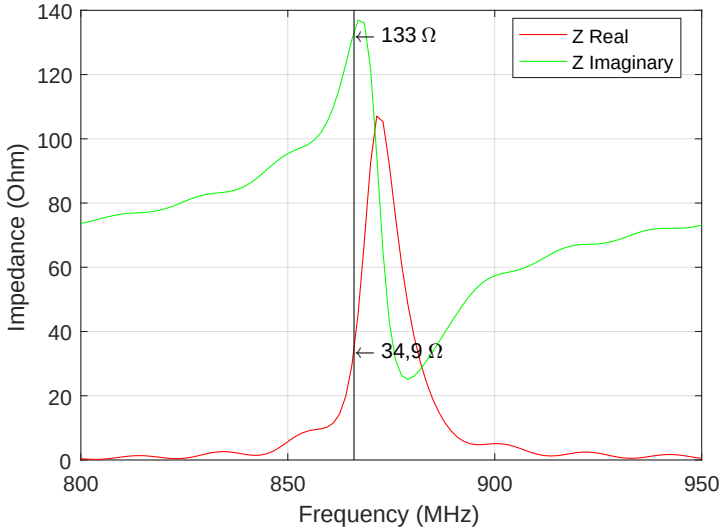

Figure 3.38: Bent dipole's input impedance.

By bending the antenna, the impedance changed to 34.9 + j133 Ω at 866 MHz. It can

then be deduced that bending has an impact on the impedance causing the antenna to be unmatched to the microchip. Figure 3.39 shows parameter S_{11} of the bent antenna.

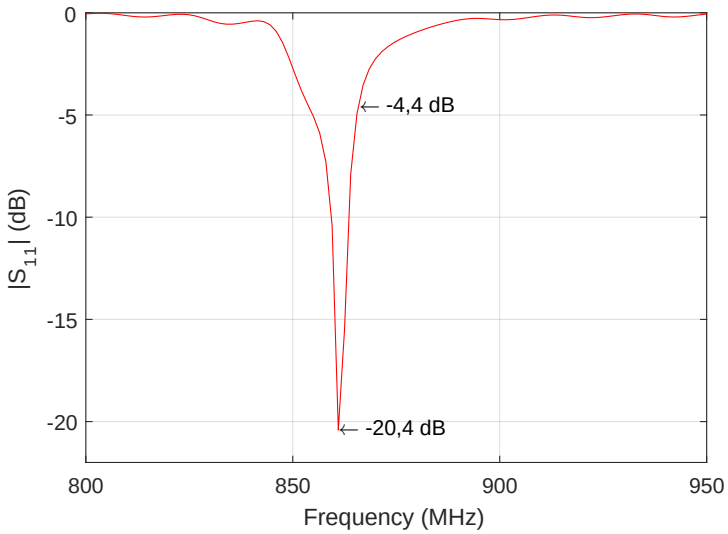

Figure 3.39: Bent dipole's S_{11} parameter.

As expected after the analyses of the impedance of this antenna, this parameter shows that the matching has also suffered a deviation. It now has a value of -4.5 dB at 866 MHz, which determines that the antenna is unmatched at this frequency. The minimum value is now -20 dB at 861 MHz. Regarding the bandwidth, it has kept its nominal value of approximately 4 MHz, but it is now between 859 MHZ and 863 MHz. Bending the antenna has a great impact of the operating frequency (which decreased from 867 MHz to 861 MHz) although a good match is observed at this new frequency. Given what was learned during the parametric study, the antenna can now be retuned by adjusting the correct dimensions. Since the antenna is to be applied on a glass bottle filled with liquid, which will certainly also unmatch the antenna, not attempt to retune the antenna will be performed here.

3.4 Meandered tip loaded dipole

Although a free space matched antenna design is already achieved, it is decided to create another antenna design. This decision is derived from the fact that the previously created antenna has a complex shape which makes its matching more complex to achieve. Furthermore, none of its dimensions have an independent variation on the impedance. That is, any variation in any of its dimensions generates a large variation

in both the real and imaginary parts of the impedance, which again makes matching difficult.

The chosen antenna for this second design is a meandered dipole with an inductive ring that is adapted in free space to the LXMS31ACNA-010 microchip which as an impedance of $Z = 12 - j107\ \Omega$ at 866 MHz [33] [30]. Figure 3.40 shows the format of the antenna chosen as basis. Its dimensions are presented in the table 3.5.

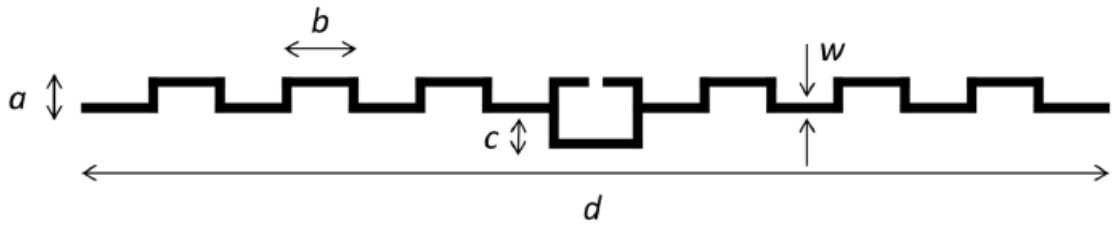

Figure 3.40: Selected RFID antenna. (extracted from [33].)

Table 3.5: Dimensions of selected RFID antenna from [33].

Parameter	**a**	**b**	**c**	**d**	**w**
Dimension [mm]	6.2	13.4	6.2	180.3	1.7

As can be seen, this antenna has a total length of 18.03 cm and a height of 1.24 cm. The maximum limits of 6 cm by 3 cm previously assumed are still taken into account so it is necessary to reduce the antenna size drastically. Although in [33] there's no mention about the impedance value of the antenna, it is specified that it has a minimum return loss value of -26 dB at the frequency of 860 MHz. Figure 3.41 shows the antenna in the simulation environment, as well as its dimensions.

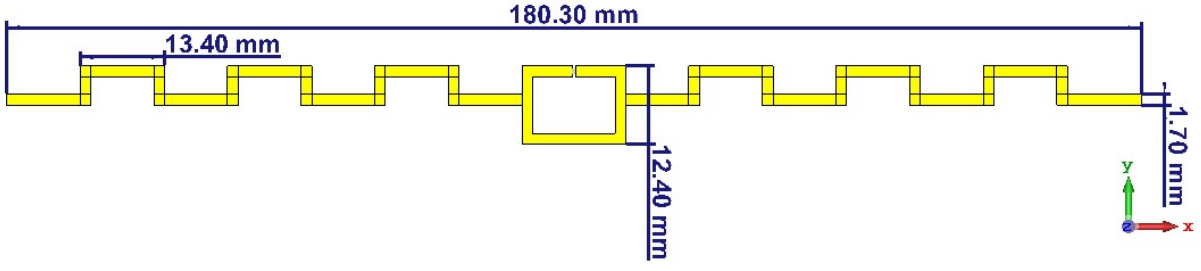

Figure 3.41: Chosen meander dipole.

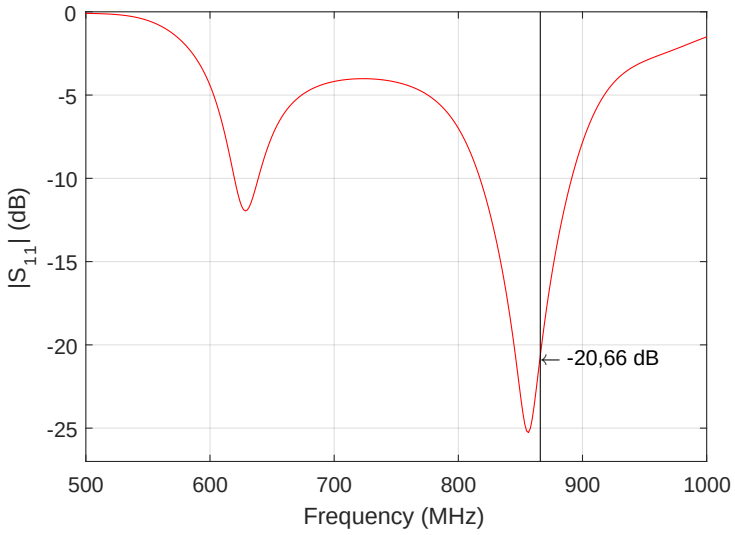

Figure 3.42: Chosen meander dipole return loss coefficient.

An impedance of 10.57 + j100 Ω at 866 MHz was obtained. Remembering that the ideal impedance of an RFID antenna is to be the conjugated complex of the IC impedance and that the microchip impedance is 12 - j107 Ω, it can be concluded that this impedance is close to the ideal value. From figure 3.42 the value of $|S_{11}|$ can be observed. Having a value of -20.7 dB at 866 MHz, proves that the antenna is adapted to the microchip.

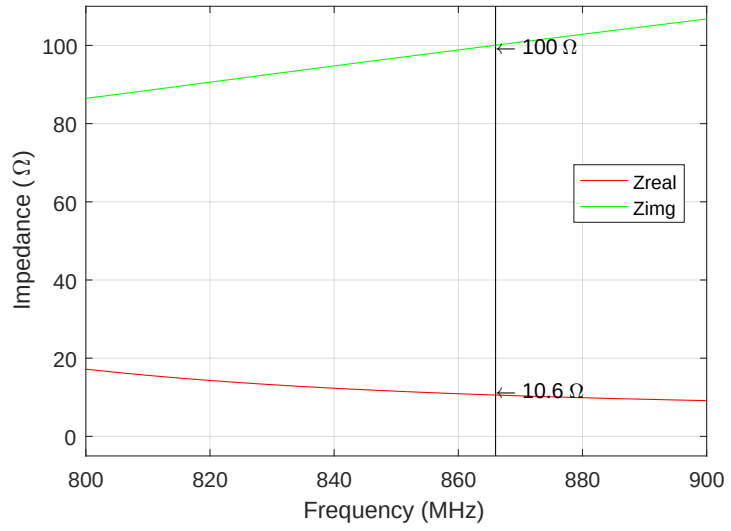

Figure 3.43: Chosen meander dipole impedance.

It is now necessary to modify this antenna to reduce its size. It is also necessary to define which microchip will be used in this dissertation. For this purpose a commercially

available RFID microchip working in the UHF RFID frequency band 865-868 MHz is chosen; the SL3S1013FTB0 from NXP Semiconductors which has an input impedance of 27 - j234 Ω at 866 MHz [34].

3.4.1 Antenna size reduction

With a chosen microchip and its input impedance defined, the size of the antenna is now reduced in order to conform with the established dimensions and assure that it is matched to the IC in a free space. A study is made of how its dimensions influence its impedance. Taking into account that this antenna is also a meander dipole, the conclusions previously drawn from the previous antenna are still applicable. The dimensions of the central inductive ring are first adjusted since, as concluded before, it is the component whose dimensions most influence the impedance of the antenna. Simultaneously, the arms of the dipole are shortened, removing some of the meander segments, in order to reduce its size. With the changes made, the antenna matched to the new microchip can be seen on figure 3.44.

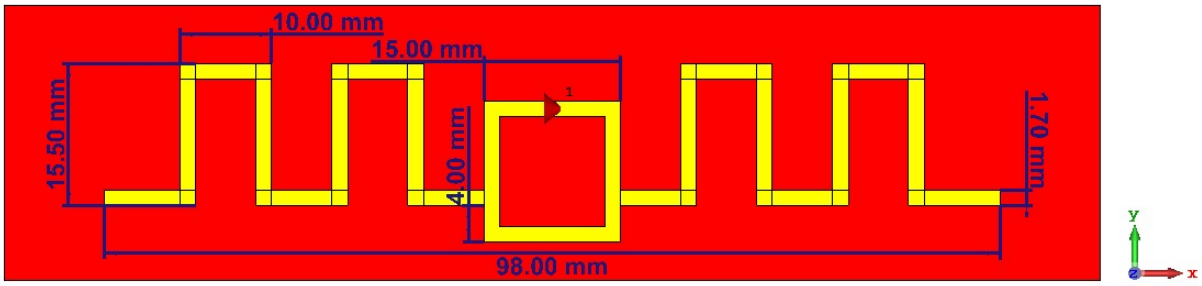

Figure 3.44: Meandered dipole and adaptation to new microchip.

By looking at the antenna in figure 3.44 it can be seen that the antenna now has a total length of 9.8 cm and a height of 1.55 cm. Although these measures still do not fit the established limits, a decrease in length of almost half is achieved without the need to increase its height drastically. The antenna is now also matched to the new microchip, having an impedance value of 34.9 + j238.15 Ω and a return loss value of -16.9 dB at the frequency of 866 MHz.

To further reduce the size of the antenna the Tip Loading technique [25] is used. Figure 3.45 shows the new adjustments made on the antenna.

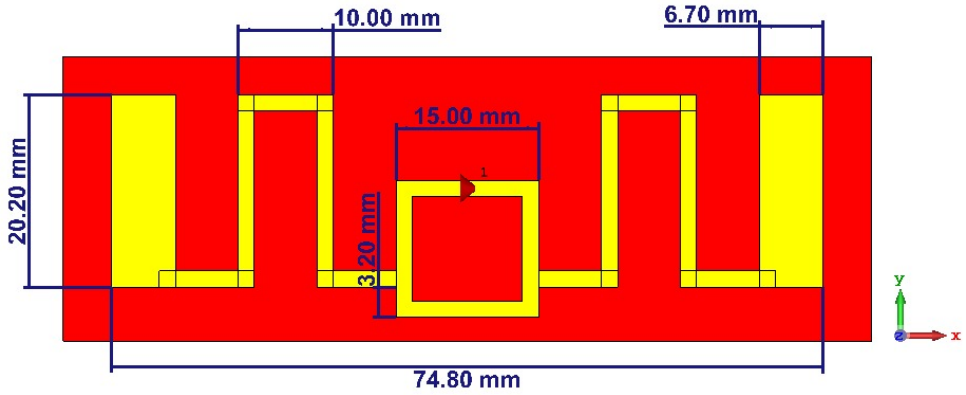

Figure 3.45: Size reduction of meandered dipole.

As can be seen in figure 3.45, a reduction of approximately 2.3 cm in antenna length is achieved although increasing its height from 1.55 cm to 2.02 cm. The side ends of the antenna now have a larger portion of copper. In figure 3.46 it can be seen that the reflection coefficient is -55.5 dB at 867 MHz. The antenna has a bandwidth of 17 MHz, between 859 MHz and 876 MHz.

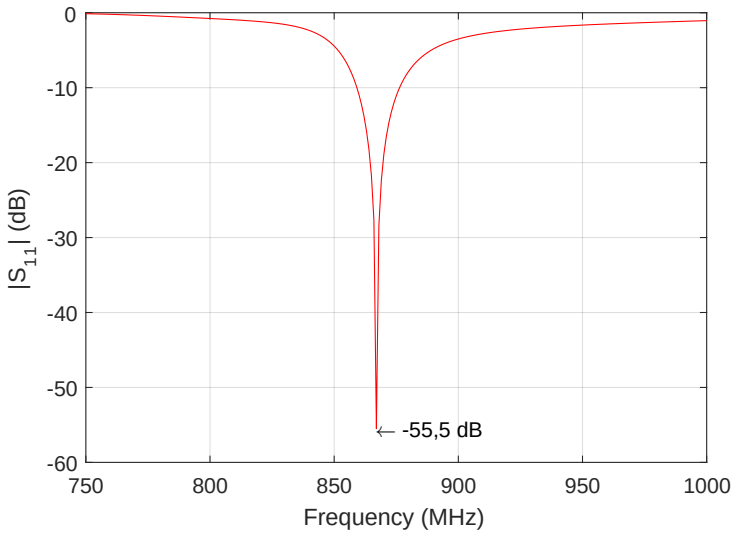

Figure 3.46: S_{11} parameter of meandered dipole.

Although the total length of the antenna is not yet within the established limits, it is decided to proceed with this antenna to test the introduction of glass and water due to the anticipation of the need to reduce its dimensions for later adaptation to the presence of these materials. This antenna is chosen over the first design created since it has a better $|S_{11}|$, a less complex shape and a smaller area overall.

4

RFID tag antennas applied on bottles

In this chapter the design of an UHF RFID antenna adapted to a bottle is presented. First, a meandered dipole already matched for free space to a certain IC is studied and adjustments are made in order to greatly reduce its size. The dipole behaviour in the presence of glass and water is then evaluated. Two models are utilized: a flat model of a layer of glass followed by a layer of liquid and a cylindrical model of the same materials mimicking a bottle. Finally, return loss tests are performed simulating the variation of different dimensions of the bottle, positions of the antenna in the bottle and different permittivities of the materials involved.

4.1 Glass influence

In order to test the effects caused by glass and water, blocks of these materials are now introduced. For simulation purposes it is defined that the length of these blocks is twice the length of the tag, with the height being three times the height of the tag, as shown in figure 4.1. The glass material is already defined in CST library having $\varepsilon_R = 6$ and $tan\delta = 3.46e^{-12}$ at 866 MHz.

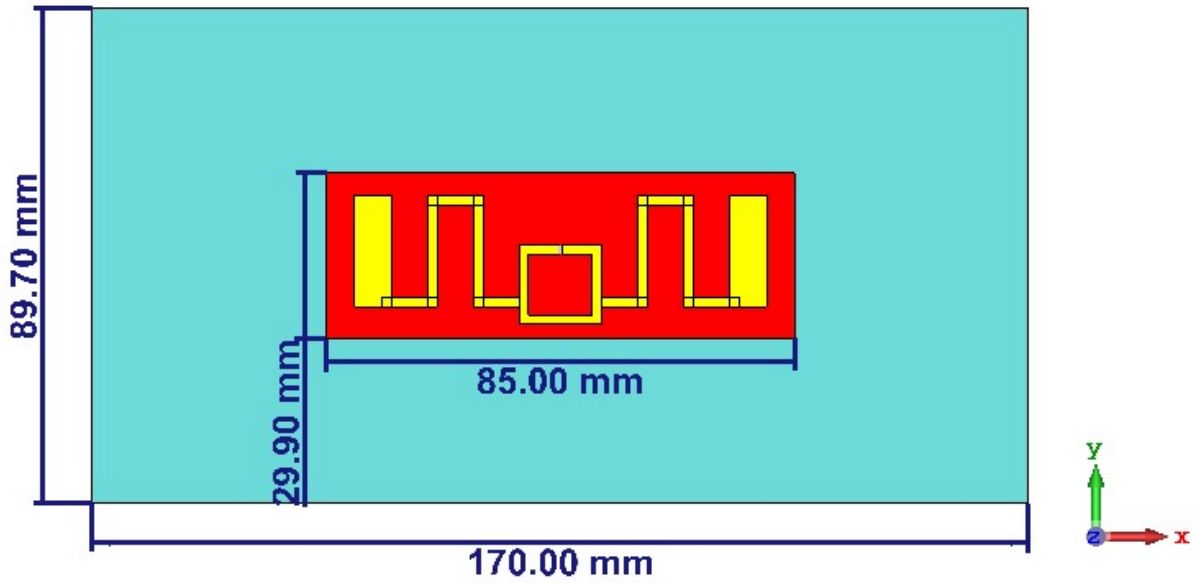

Figure 4.1: Meandered dipole applied to glass block.

The blue block in figure 4.1 represents the glass block. The thickness initially defined for this block is 2 mm, being this the typical thickness of a glass bottle [20]. The return loss parameter can be seen in figure 4.2.

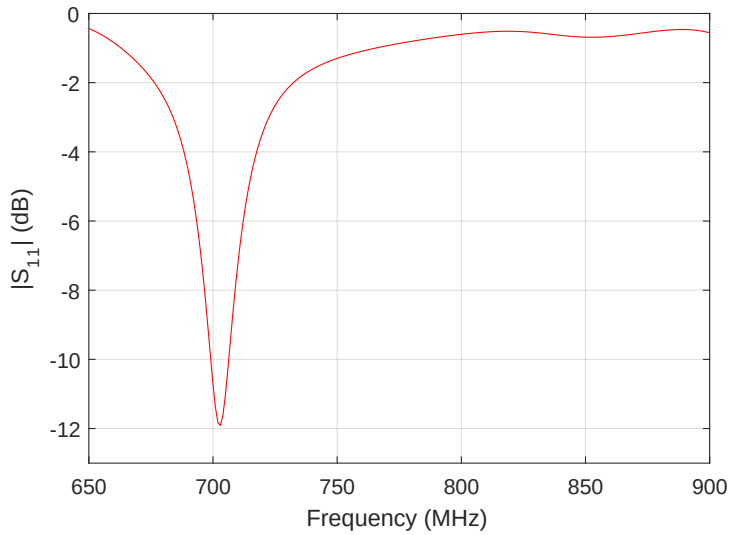

Figure 4.2: $|S_{11}|$ parameter of meandered dipole with glass block influence.

As expected, the introduction of the glass greatly alters the antenna input match. The minimum value of the $|S_{11}|$ has changed from 867 MHz to 703 MHz, making the antenna completely unmatched in the UHF RFID operating band. In addition, the nominal value of this parameter has also degraded, changing from a value of -55.5 dB to

-11.9 dB. In order to match the antenna on glass, changes are made on the dimensions of the antenna starting with the center ring. Figure **??** shows the new antenna.

Comparing figures 3.45 and 4.3, the length is reduced by 2.5 cm, making the antenna a total length of approximately 5 cm. In relation to its height there is a slight reduction, remaining practically unchanged. There is a reduction both in the size of the meandered arms of the dipole and also in the length of the tip loading.

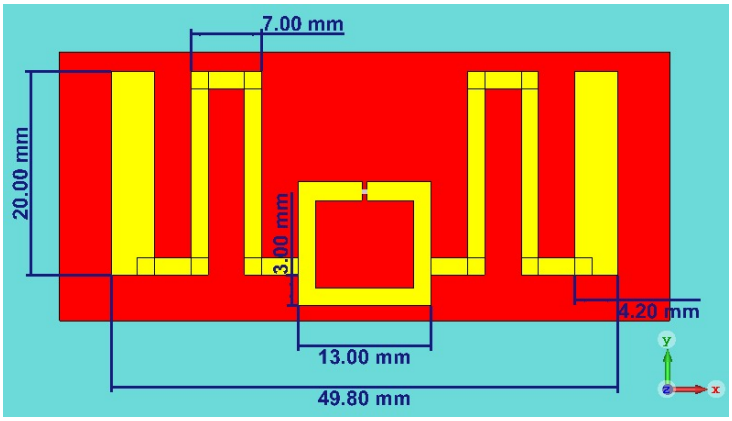

Figure 4.3: Meandered dipole adapted to glass block.

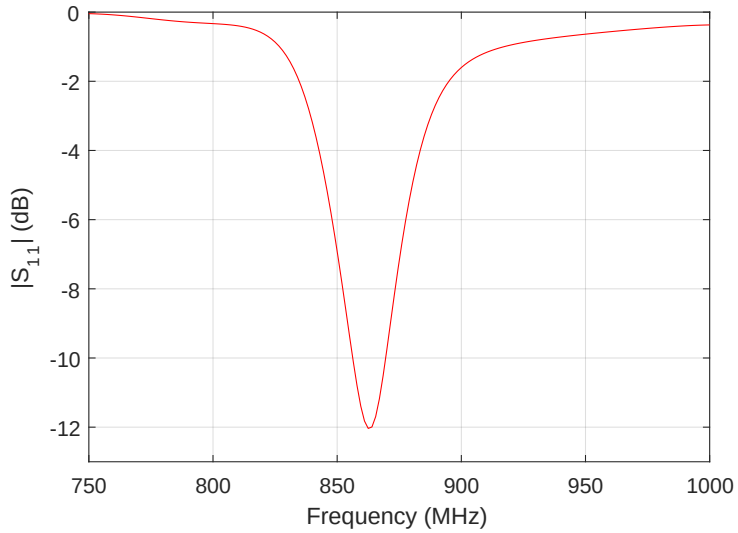

Figure 4.4: $|S_{11}|$ parameter of meandered adapted to glass block.

Regarding input matching, and seen in figure 4.4, there is a degradation in the nominal value of the return loss when compared to the previous antenna matched on the free space. This parameter has a minimum value of -12 dB at 862.5 MHz frequency. At 866

MHz its value is -11.5 dB. The bandwidth has decreased to 13 MHz, between 856 MHz and 869 MHz.

In order to understand how much the antenna input match (or its impedance) changes with bottle thickness, a test is now performed varying the thickness of the glass block. In figure 4.5 it is possible to see the $|S_{11}|$ parameter as function of glass block thickness.

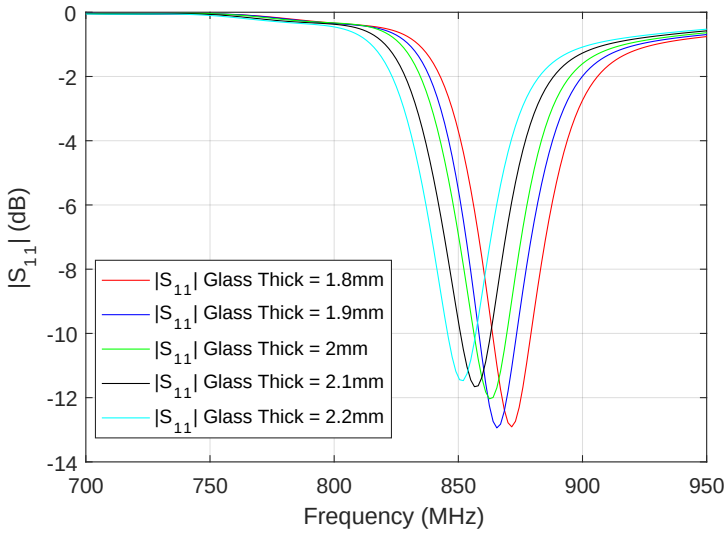

Figure 4.5: $|S_{11}|$ parameter variation with glass block thickness.

As can be concluded, a minimum variation of 0.1 mm in the thickness of this material causes considerable changes in antenna's input match. Interestingly, the antenna is best matched to a glass thickness of 1.9 mm with an $|S_{11}|$ value of -12.9 dB. However, this value quickly becomes degraded with minimal increase or decrease of this thickness. For an increase of 0.1 mm, and the thickness value becoming 2.1 mm, the antenna is already unmatched with a reflection coefficient value of -8.5 dB. With a reduction of 0.3 mm in thickness, the antenna also becomes unmatched, having a $|S_{11}|$ value of -8.26 dB.

With this test it is concluded that the thickness of the bottle where the antenna will be applied has a great influence on its performance. In practice, it may be difficult for this tag to work on another bottles.

4.2 Water influence

Simulations are now carried out concerning the introduction of water. For this, a 10 mm thick block of water is created with an area identical to the one created for glass. The dielectric properties of water in CST library are defined in figure 4.6, having an

$\epsilon_R = 78$ and $tan\delta = 0.423$ at 866 MHz. The glass block is kept present to account for its effect, thus making the simulation more realistic. The introduction of the water block can be seen in figure 4.7.

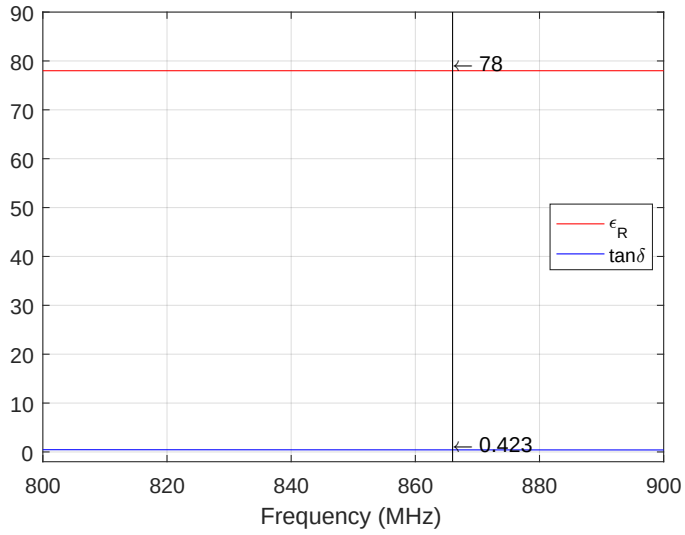

Figure 4.6: Dielectric properties of water in CST.

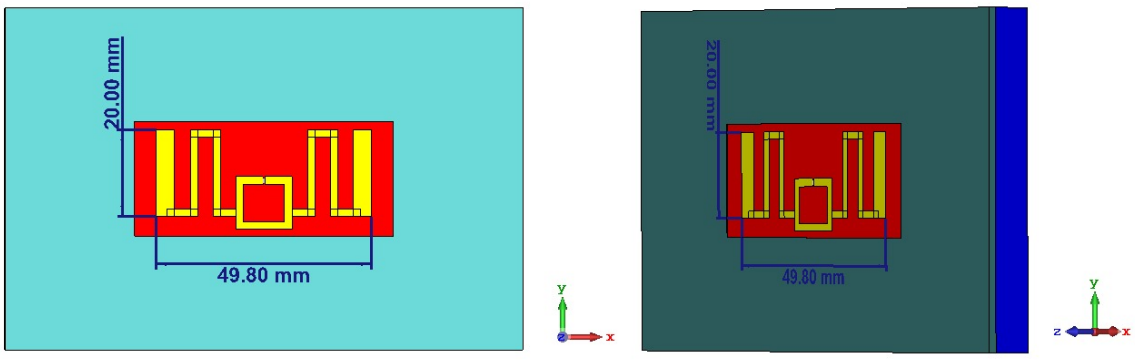

Figure 4.7: Antenna adapted to glass with water block.

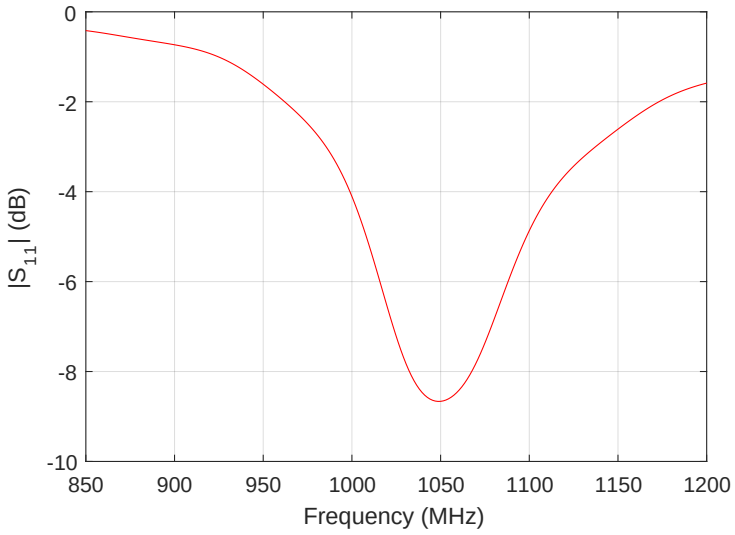

Figure 4.8: S_{11} parameter of the antenna adapted to glass with water block influence.

In figure 4.8 the antenna's return loss values can be observed. As expected, it became unmatched, having the minimum value of $|S_{11}|$ of -8.6 dB at 1048 MHz. Given this, more changes are now made to the antenna to adapt it to the effect of the water. Figure 4.9 shows the antenna already adapted to the water as well as its dimensions.

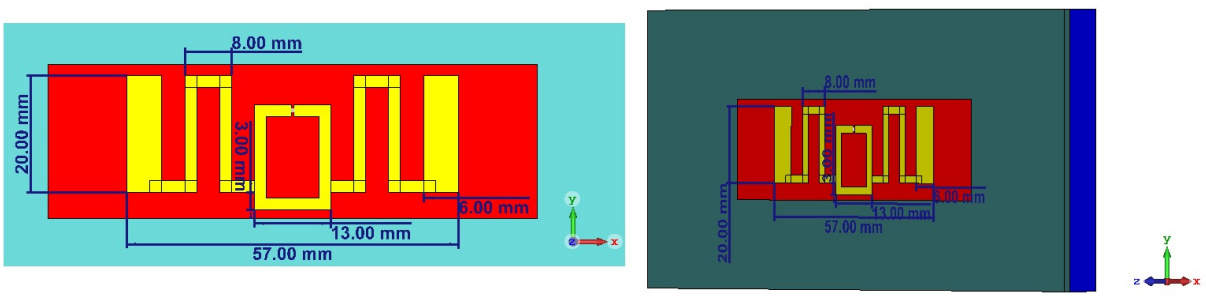

Figure 4.9: Antenna adapted to glass and water presence.

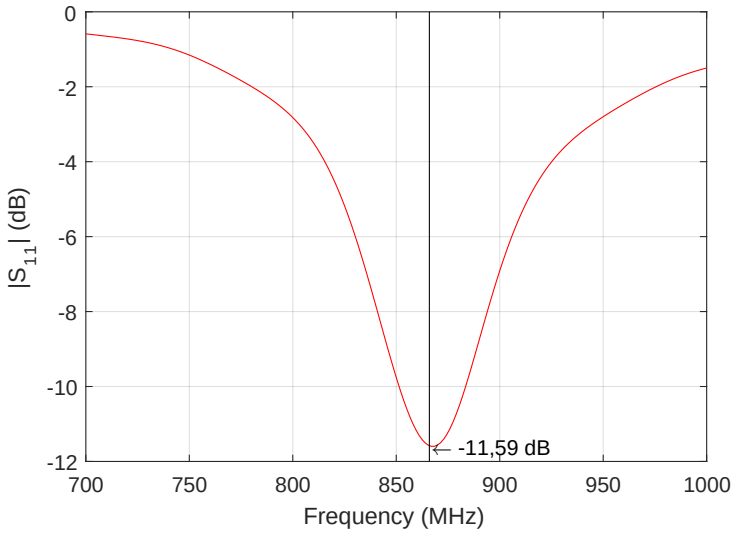

Figure 4.10: Return loss of antenna adapted to glass and water influence.

When compared to the previous antenna, it can be concluded that it has increased its length by about 0.7 cm. Despite this increase, the antenna still remains within the established limits. There were no changes in the height of the antenna, keeping it at 2 cm. By looking at figure 4.10, it can be seen that the antenna is matched, having a minimum value of $|S_{11}|$ of -11.6 dB at 867 MHz.

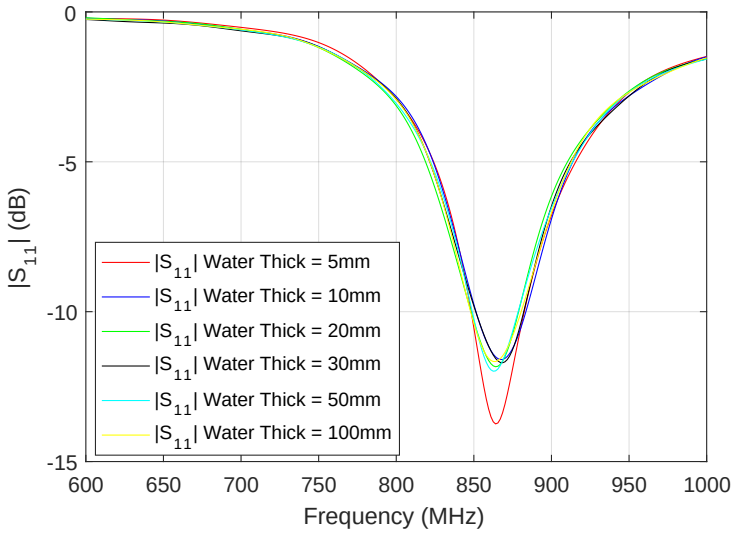

Figure 4.11: $|S_{11}|$ parameter variation with glass block thickness.

Similar to what was done for the glass block, the effect of variation in the thickness of the water block is now studied. This test is intended to understand if the quantity of

the water layer influences or not the antenna. Analyzing figure 4.11 it can be concluded that varying the water layer does not seem to greatly influence the antenna's matching, since it can be seen that by reducing the water density to 5 mm, or even increasing it to 10 cm, the reflection coefficient values do not go below -11.5 dB, assuring that for any thickness value in this range the antenna is always well matched.

4.3 Bending effect

Although a model of the antenna matched to the presence of glass and water has already been achieved, the effect of bending the antenna has not yet been addressed. To test this, the action of bending the four constituent materials is now applied: the copper that composes the antenna, the paper where the antenna is applied, glass and water. It should be noted that the thickness of glass and water are respectively 2 mm and 10 mm for this simulation, as this were the dimensions that the antenna was matched to. Figure 4.12 shows the antenna and the materials already with the bend effect introduced.

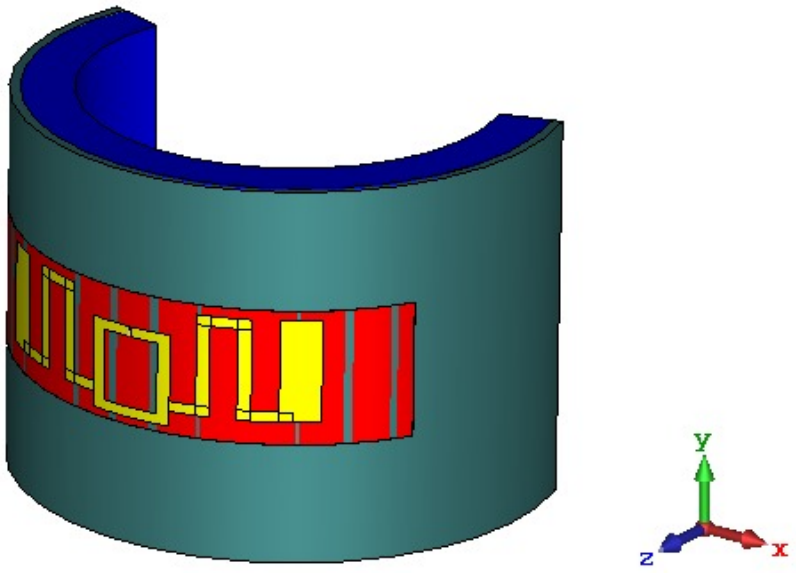

Figure 4.12: Antenna with bend effect.

It is important to emphasize that the bending radius applied to the materials are related to commercially used glass bottles which are approximately 8 cm in diameter. By analyzing figure 4.13 it can be deduced that there is a relevant unmatching of the antenna when it is bent.

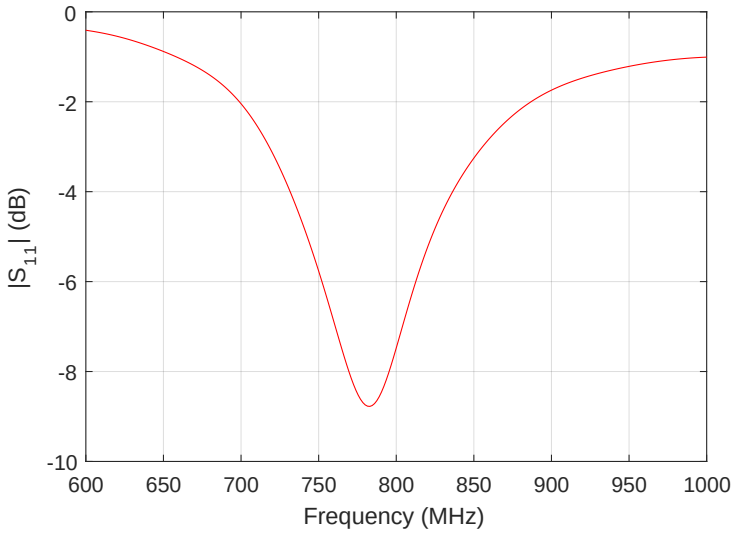

Figure 4.13: Antenna with bend effect.

4.4 Tag for realistic bottle

A bottle is now chosen on which an antenna will be later applied. Several glass bottles dimensions were measured and the one with dimensions closer to those previously taken into account was chosen. The chosen bottle and the measurements made can be observed in figures 4.14 and 4.15.

Figure 4.14: Bottle diameter measurement

Figure 4.15: Bottle thickness measurement

The measured diameter of the bottle is approximately 7.1 cm, and the thickness of the glass is 2 mm. These are the measurements with which a model of the bottle body is created in the simulation environment. A cylindrical hollow glass block representing the bottle is created with the 2 mm thickness. Inside this block, a cylindrical water block is created, simulating a bottle full of liquid. The antenna is then applied centered on the surface of bottle, as shown in figure 4.16.

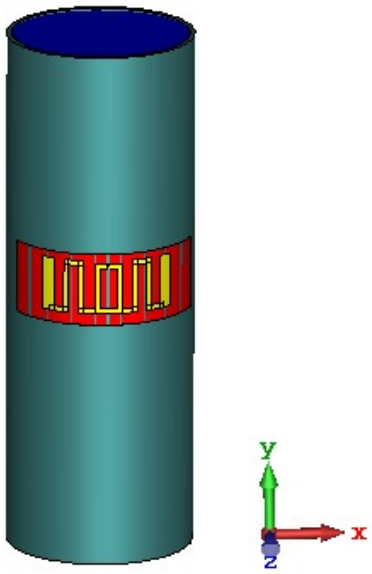

Figure 4.16: Antenna applied on simulated bottle.

The bottle has a height of 20 cm and a diameter of 7.1 cm. The antenna previously designed is placed on the bottle. New adjustments were made in order to retune the antenna to the desired frequency. The new dimensions are shown in figure 4.18 which resulted in the $|S_{11}|$ shown in figure 4.17. It has a minimum value of -14.53 dB at 868.5 MHz, and a value of -14.8 dB at 866 MHz. The input impedance is 38.5 + j229.6 Ω, which when compared with the impedance of the microchip still shows some deviation in the real part.

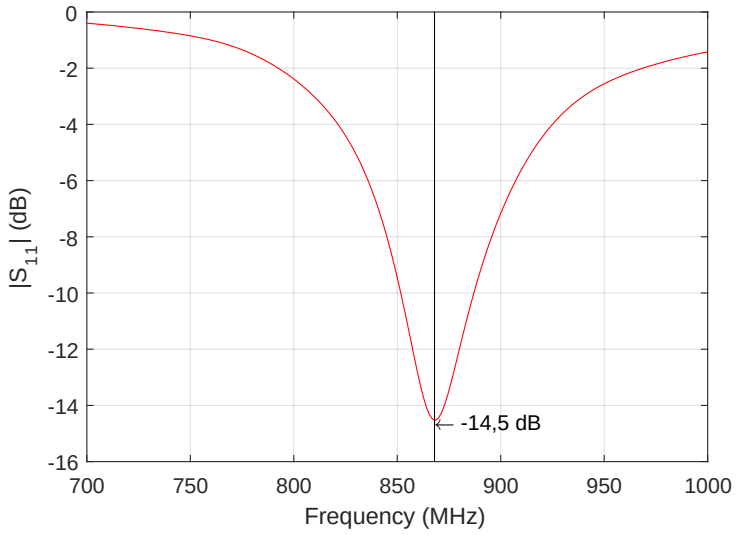

Figure 4.17: $|S_{11}|$ parameter of antenna applied on simulated bottle.

The bandwidth has a value of 34 MHz, between 852 MHz and 886 MHz.

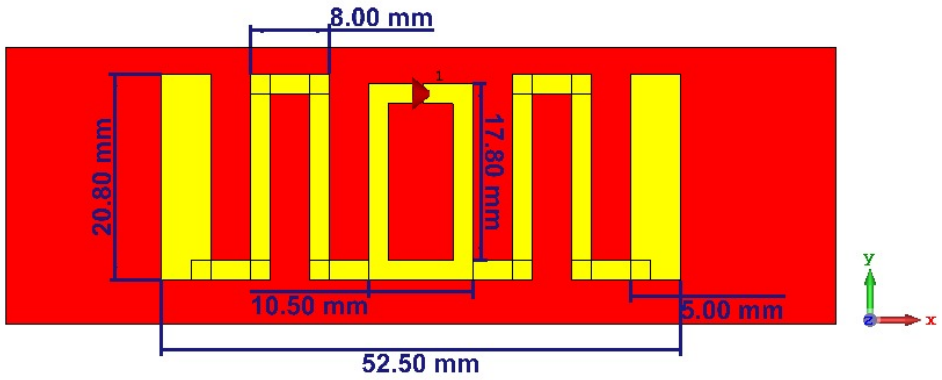

Figure 4.18: Antenna applied on simulated bottle dimensions.

The 3D gain radiation pattern of the antenna can be seen in figure 4.19. The polar representation of its pattern is shown in figures 4.20 and 4.20, while the current density is in figure 4.22.

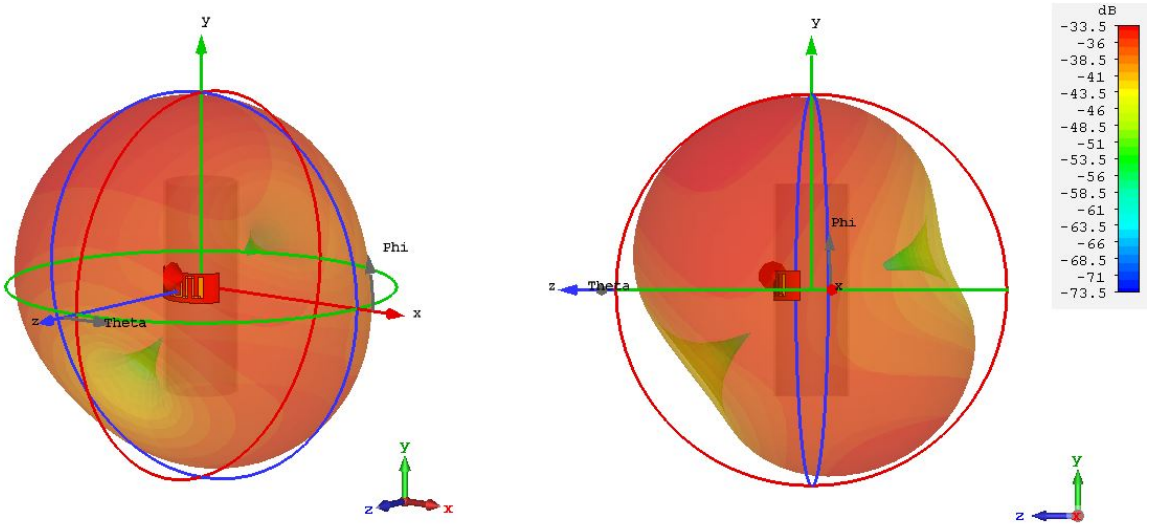

Figure 4.19: Antenna's 3D gain radiation pattern.

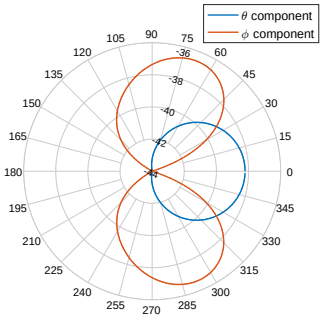

Figure 4.20: Antenna's polar gain radiation pattern at plane XZ.

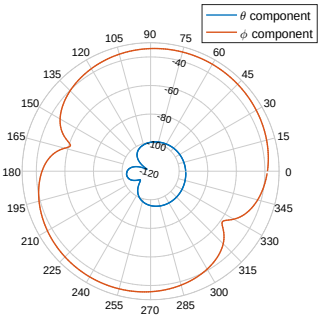

Figure 4.21: Antenna's polar gain radiation pattern at plane YZ.

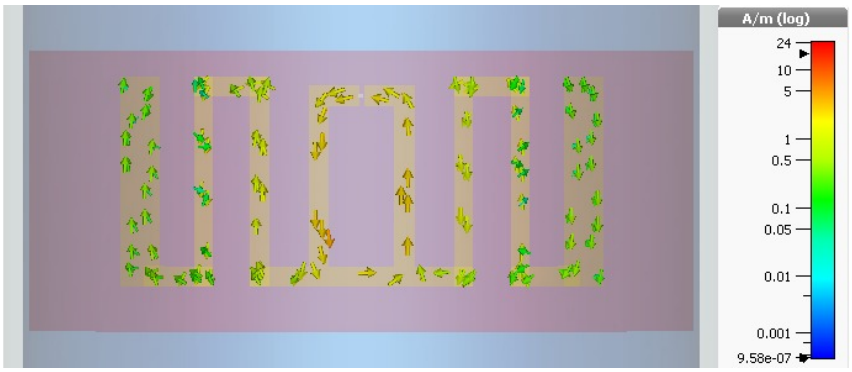

Figure 4.22: Antenna's current density.

As shown in figures 4.19, 4.20 and 4.21 the antenna has a non directive radiation diagram and can, theoretically, be detected in a 360º radius. It is noticeable in figure 4.22 that the current distribution follows the typical current distribution of a dipole, with it's highest value at the center (near the feeding point) and decreases as it approaches the dipole ends.

On table 4.1, a comparison between the initially antenna (the free-space antenna) and the bottle antenna is made.

Table 4.1: Comparison between the three antennas.

	Length	Height	Impedance	S_{11} @866 MHz
Inicial chosen antenna	18.03 cm	1.24 cm	12.7 + j109.2 Ω	-20.7 dB
Free Space antenna	7.48 cm	2.02 cm	34.9 + j238.2 Ω	-27.7 dB
Bottle adapted antenna	5.25 cm	2.08 cm	38.5 + j229.6 Ω	-14.8 dB

Between the initial antenna and the free-space antenna a reduction of approximately

10.5 cm in length was achieved with only a 0.8 cm increase in height. In addition an improvement of -7 dB in the matching level of the antenna was also achieved by decreasing $|S_{11}|$ from -20.7 dB to -27.7 dB. Comparing the impedance of these two antennas has no meaning since the microchips used in each antenna have different impedances. Analyzing the bottle adapted antenna it can be concluded that it has a length of approximately 2.2 cm smaller when compared to the free space antenna, with almost the same height. As for the $|S_{11}|$ parameter it presents a value of -14.8 dB which is not as good as the $|S_{11}|$ value of the free space antenna. However, this antenna is theoretically capable of operating in a glass bottle with water, materials which impact the performance of the antenna and reduce the nominal value of this parameter.

By analyzing figure 4.19 it can seen that the pattern is quite similar in all directions, with the exception of the rear back and the bottom of the bottle, where a large decrease in the antenna gain can be observed.

Having already obtained an antenna adapted to a bottle it is now necessary to test some deviations that may occur if the conditions for which it is adapted are not exactly met. Therefore it is decided to test the dependence of antenna matching with glass thickness of the bottle. It is important to point out that the increase or decrease of this thickness alters the volume of water present inside the bottle which also influences the performance of the antenna. However, this variation in thickness does not change the radius of curvature to which the antenna is subjected.

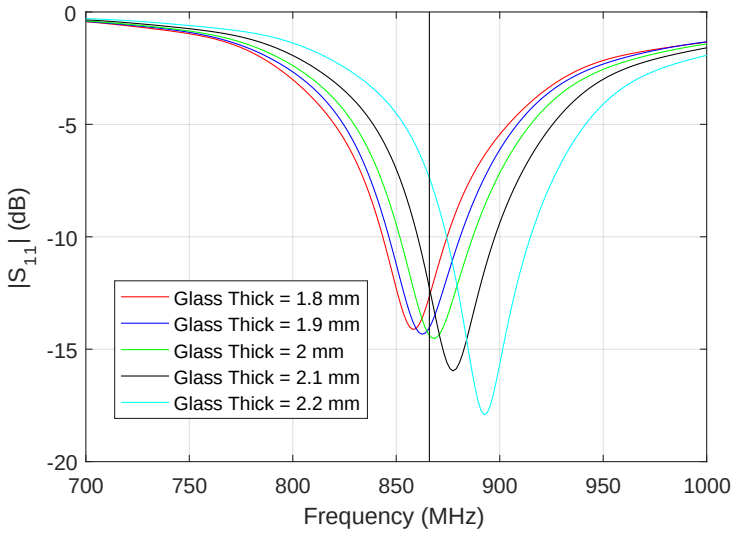

Figure 4.23: $|S_{11}|$ with glass thickness variation.

Table 4.2: S_{11} values at 866 MHz with glass thickness variation.

Glass Thickness	1,8 mm	1,9 mm	2 mm	2,1 mm	2,2 mm
S_{11} Value	-12,65 dB	-14 dB	-14,38 dB	-12,27 dB	-7,38 dB

The results obtained in the variation of tenths of millimeter in the thickness of the bottle glass can be seen in figure 4.23. The reflection coefficient of the antenna experience some deviations in frequency with the variation of this thickness. The results at 866 MHz are summarized in table 4.2. It can be concluded that with an increase of 0.2 mm in glass thickness the antenna is already unmatched, presenting a value of $|S_{11}|$ of -7.38 dB. However the same does not happen for an equal reduction in thickness, since the antenna is still adapted for a thickness of 1,8 mm. With a thickness of 1.5 mm the return loss value of the antenna is higher than -10 dB. Since glass thickness is a critical factor for antenna performance, it is unlikely that the same antenna will work in bottles of different thickness and shape.

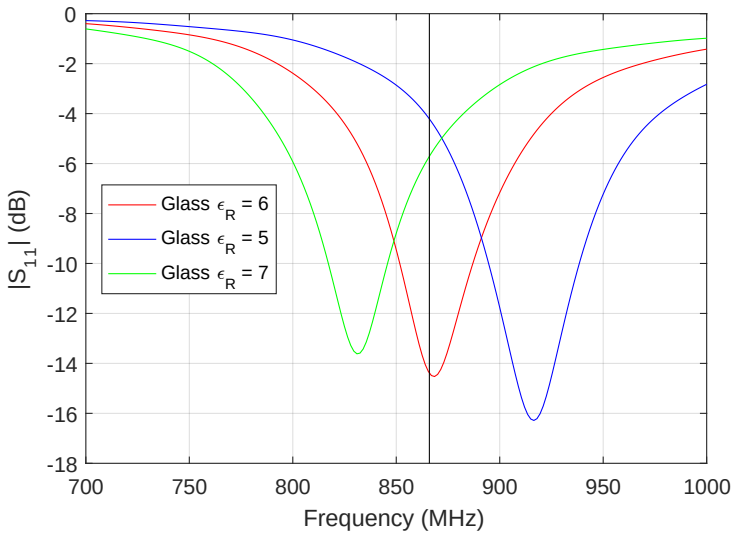

Figure 4.24: $|S_{11}|$ with glass permittivity variation.

Another important issue is the variation of the relative permittivity of glass. Up to now, the permittivity associated to the glass material was $\varepsilon_R = 6$. However, the dielectric constant of glass can vary between 3.7 and 10 [35]. As such, the variation of this parameter is simulated to analyze the variation of the antenna input match. The

results of this variation can be seen in figure 4.24. By changing the ε_R value of glass to 5 or 6 there is an unmatch of the antenna at the frequency of interest of 866 MHz.

The temperature of the water affects its permittivity [36]. With the increase of the water temperature ε_R drops, and with the decrease of temperature it increases. Although the antenna is designed to work at an ambient temperature, it is relevant to study whether the performance of the antenna changes depending on whether the water is colder or warmer. Hence, the impact of the variation of the water permittivity is now studied.

By analyzing the results of the variation of the water permittivity, presented in figure 4.25, it can be concluded that the antenna remains adapted for practically all the tested values.

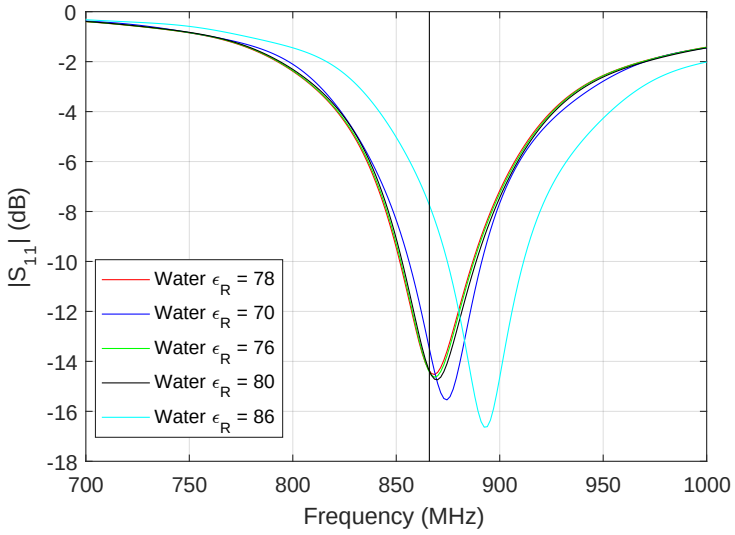

Figure 4.25: $|S_{11}|$ with water permittivity variation.

Only for ε_R of 86, which is equivalent to the water having a temperature close to 2º C, is the $|S_{11}|$ value higher than -10 dB. Therefore it can be inferred that the water's permittivity does not substantially influence the antenna's performance.

Having already been tested the variations in glass thickness and material permittivities, three antenna positions, as shown in figure 4.26, are evaluated.

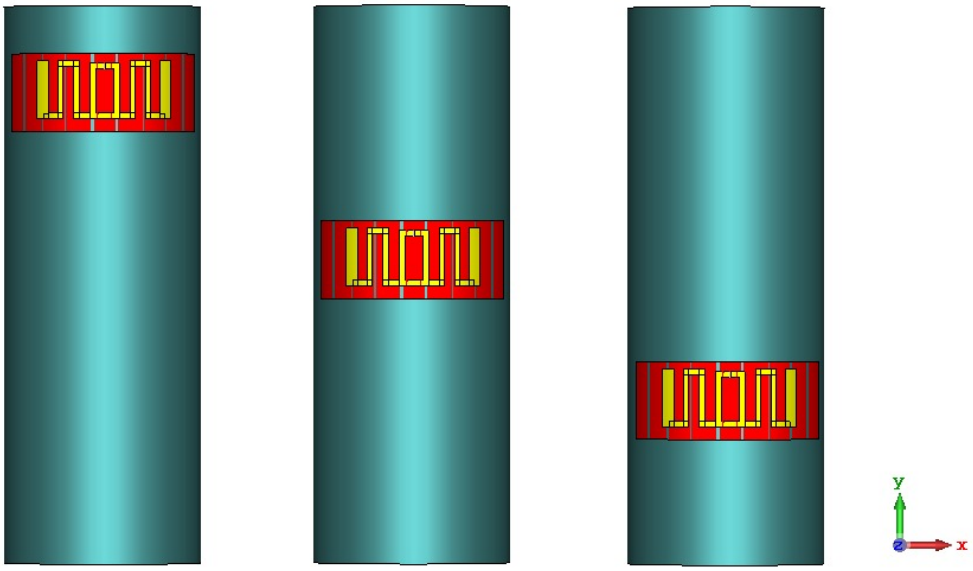

Figure 4.26: Representation of the antenna positions tested.

The results of the impedance and $|S_{11}|$ as function of antenna position are shown in figures 4.28 and 4.27, respectively. As can be seen, the position of the antenna on the bottle does not influence its impedance and therefore does not influence its input match.

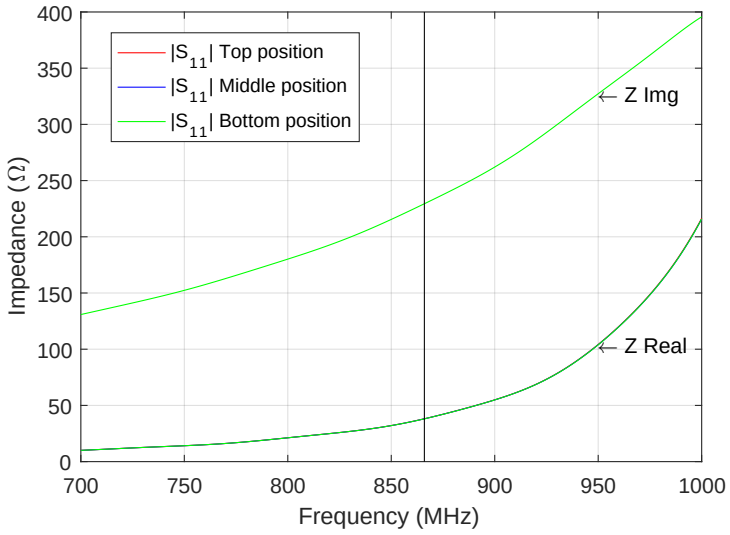

Figure 4.27: Impedance with antenna position.

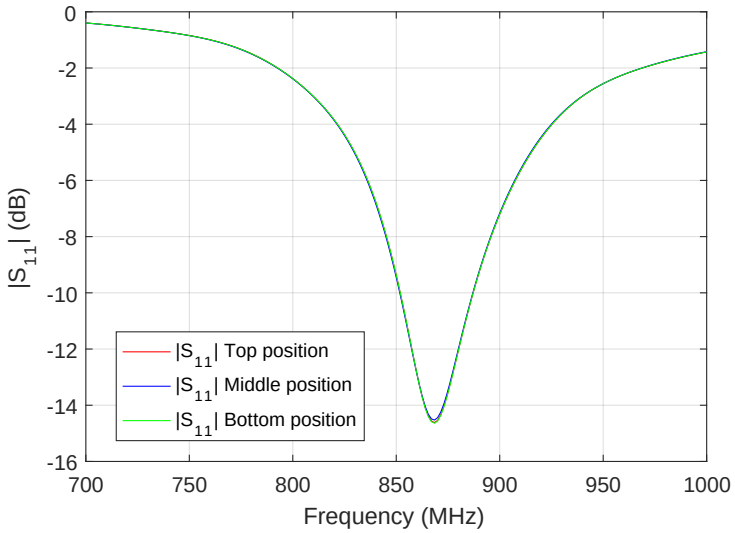

Figure 4.28: $|S_{11}|$ parameter with antenna position.

The variation in the radius of curvature is now tested. It should be noted that with this variation not only the bending radius varies but the volume of water inside the bottle also varies. The larger the radius, the larger the volume of water and vice-versa. The return loss can be seen in figure 4.29.

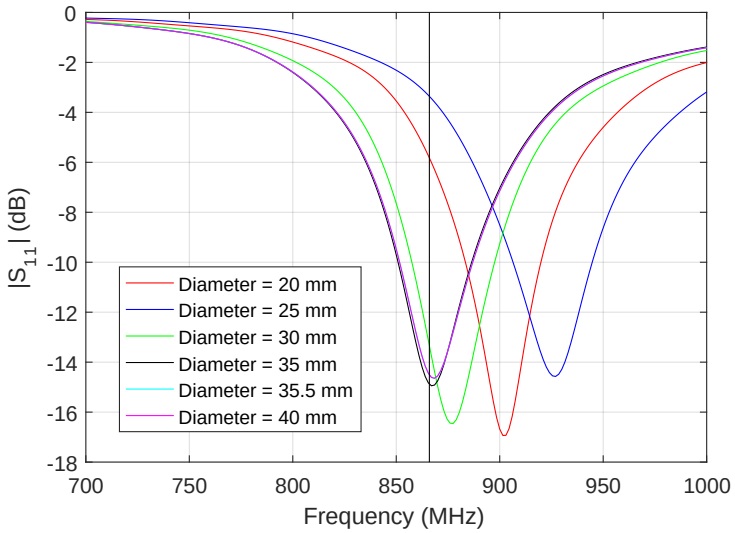

Figure 4.29: $|S_{11}|$ parameter with bottle diameter variation.

By analyzing these results it can be concluded that if the diameter of the bottle changes substantially the antenna loses matching. Even with an antenna designed to a 7 cm diameter, for a bottle diameter value of 7.1 cm the antenna maintains its adaptation with

an $|S_{11}|$ value of -14,5 dB. Even so, if this diameter has a variation of 1 cm, becoming 6 cm or 8 cm, the antenna still remains matched, presenting $|S_{11}|$ values of -13.3 dB and -10 dB, respectively. However, for a diameter of 5 cm or above 8 cm the antenna already presents a return loss higher than -10 dB.

5

Tag range measurement

In this chapter the experimental tests performed on the constructed tags are described. A RFID reader is used for these tests and the reading distance of the tags is measured in several situations such as free space, when applied to empty bottles and when applied to bottles with different liquids.

5.1 Experimental setup

To perform read range tests the Alien ALR 8800 RFID reader [**?**] is used, shown in figure 5.1. It is composed by the reader and two antennas that transmit and receive the signal to and from the tags. The kit assembly seen in the image 5.2 is the one used for testing the tags in the non-controlled environment.The antennas are placed on a surface and the tags are gradually moved away from them until they are no longer readable, thus achieving the maximum distance. The test setup for the controlled environment can be seen in figures 5.3 and 5.4. This reader identifies tags using the EPC Gen 2 protocol [**?**], also known as ISO Protocol 18000-6C, compatible with the microchips used in the tags. It has a RF power of 2 W ERP [**?**] and operates in the frequency range of 865.6 MHz to 867.6 MHz.

Several tests are carried out to obtain the maximum tag reading distances. Each of these tests is performed in two different environments. In a controlled environment, a small anechoic chamber is used to eliminate as many reflections as possible in order to make measurements free space like. In a non-controlled environment, tag readings are

performed without any electromagnetic shielding. However, it is ensured not to carry out the tests near metals or other highly reflective materials.

In the figures 5.1 and 5.2 the RFID reader kit can be seen.

Figure 5.1: RFID Reader.

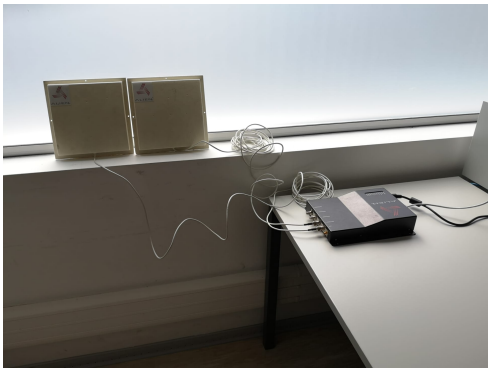

Figure 5.2: RFID Kit - Reader and antennas.

Figure 5.3: Controlled environment setup for tag testing.

Figure 5.4: Controlled environment setup for tag testing.

The antennas of the RFID reader are mounted on a platform that can be moved horizontally and vertically, thus allowing for the distance and alignment tests.

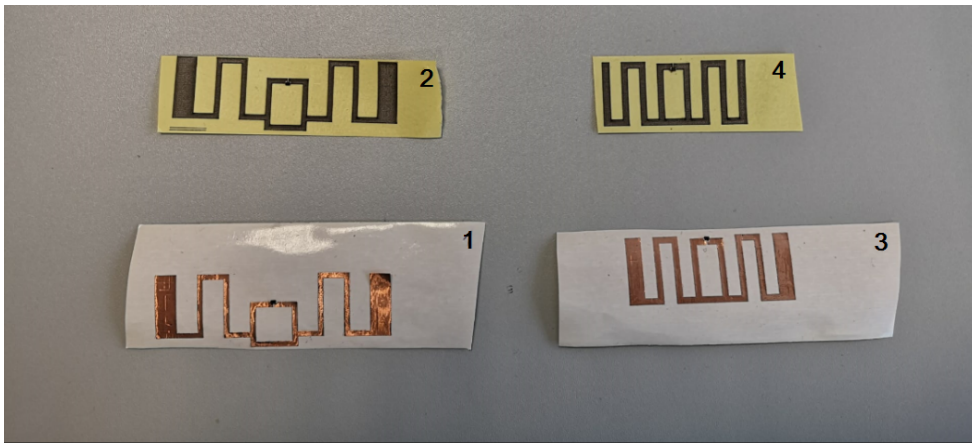

Figure 5.5: Constructed tags.

The four constructed tags can be observed in figure 5.5. The tags on the left, numbered 1 and 2, are the tags designed to work in free space. On the other hand, the antennas on the right side, numbered 3 and 4, are the ones designed to work on a bottle filled with water, whose antenna model is the one in figure 4.18. The difference between the antennas with the white and yellow paper base is the manufacturing material. Antennas 2 and 4 were made with a with a fabric tape containing nickel, copper and cobalt, that has a resistivity of less than 0.1 Ω/sq and a thickness of 0.127 mm. Antennas 1 and 3 were manufactured with a copper foil tape, which has a resistivity of 0.005 Ω/sq and a thickness of 0.04 mm.

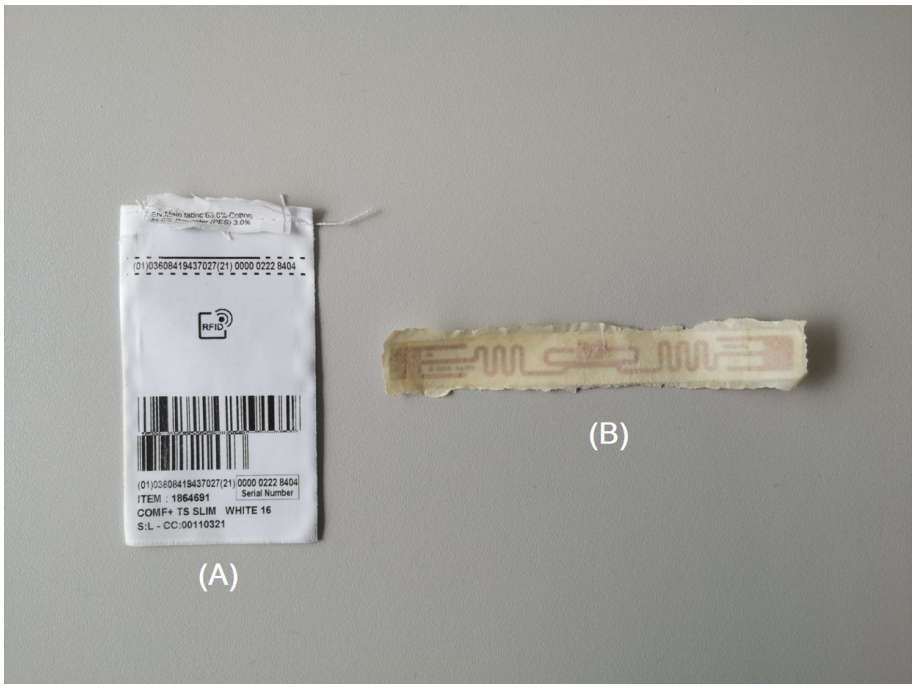

Figure 5.6: RFID commercial tag (A) and RFID Alien tag (B)..

Figure 5.6 shows two other tags also used in the tests for comparison purposes. The

tag in figure **??** is a commercial tag while the tag in the figure **??** is a tag from the alien RFID reader kit. The tests performed are based on the measurement of the maximum reading distance at which the tags can be identified by the reader.

In the free space scenario, two different tag placements are investigated: flat e bent. In both cases, the tags are placed on styrofoam (which has a permittivity close to air).

5.2 Free space scenario

Although two of the four constructed tags were designed to be on a bottle with water, they are also contemplated in these tests to evaluate their behavior in this environment, and to compare the efficiency between the two types of tags, free space and bottle adapted.

The first free space test is performed with the tags as flat as possible, so that the effect of bending the tag is not influencing the test. In the non-controlled environment each of the tags start by being placed close to the RFID reader's antennas and are gradually moved away until they are no longer read, thus being able to get the maximum reading distance at which they can be read. In the controlled environment the tags are placed on a styrofoam support since this material has no influence on the electromagnetic signals. Then the tags are placed inside the anechoic chamber and the reader antennas are first placed at the entrance of the chamber and are gradually moved away until the maximum reading distance of the tags is found. It should be noted that in this experiment test the reader antennas are aligned with the tag being tested, since vertical variations between the tags and the antennas can influence the measurements. The results of the first test in free space can be seen in the table 5.1.

Table 5.1: Free space flat tag test results.

2***Tag**	**Maximum read distance**	
	Non-controlled	**Controlled**
Tag1	55 cm	57 cm
Tag2	125 cm	157 cm
Tag3	80 cm	90 cm
Tag4	15 cm	15 cm
Commercial tag	160 cm	240 cm
Tag Alien	10 cm	20 cm

It can be concluded that the tags built for this environment, tags 1 and 2, have shown a good performance since both are able to be read at a distance superior than half a meter.

Surprisingly, the tags designed to work on a bottle with water can also be read, with tag 3 reading a maximum distance of 90 cm in the controlled environment, which exceeded the reading distance of tag 1. The commercial tag has the longest reading distance with 240 cm. The Alien tag could only be read at 20 cm. The differences in reading distances between the test environments do not differ greatly, with the exception of the commercial tag which increased the distance by 80 cm when compared to its maximum distance obtained in the uncontrolled environment.

The second free space test is done by slightly bending the tags in order to evaluate the influence of this effect on their reading distance. On the non-controlled environment the tags are first folded against a bottle, and then the bottle is removed and the tag is gradually moved away from the antenna as in the first test, while keeping it folded. A piece of styrofoam with the bottle radius is cut to attach the tags to be tested in the controlled environment as shown in figures 5.7 and 5.8.

Figure 5.7: Top view of styrofoam for bent tags.

Figure 5.8: Front view of styrofoam for bent tags.

Table 5.2: Free space bent tag test results.

2***Tag**	**Maximum read distance**	
	Non-controlled	**Controlled**
Tag1	45 cm	42 cm
Tag2	55 cm	135 cm
Tag3	75 cm	74 cm
Tag4	10 cm	Not read
Commercial tag	100 cm	111 cm
Tag Alien	Not read	Not read

The table 5.2 shows the results of this test. For tag 1 the maximum reading distance decreased by 10 cm on the non-controlled environment and 15 cm on controlled environment, to a maximum distance of 45 cm and 42 cm respectively. For tag 2 the

maximum reading distance dropped to around half the reading distance on the first environment, but kept nearly the same distance in the controlled test when comparing the free space tests. Although both tags have now a more similar reading distance in the first environment, tag 2 shows much better performance in the controlled environment test. It is important to note that these tags have not been designed to work while bent. When analyzing the results for tags 3, it can be seen that it is not much affected by this effect, only decreasing 15 cm, being possible to deduce that the adaptation of this tag to the bent effect was well accomplished. With the results of both free space tests it becomes evident that tag 4 performs significantly worse than tag 3. However, both of these tags are designed for a bottle with liquid in it, and it is expected that they will still be readable in that situation unlike the free space tags. The reading distance of the commercial tag dropped by half in the controlled environment. However, it is still possible to read it from over a meter away. The Alien tag could not be read in this test.

Table 5.3: Free space vertical alignment test results.

Tag	**Upside distance**	**Downside distance**
Tag1	+20 cm	-12 cm
Tag2	+40 cm	-30 cm
Tag3	+28 cm	-23 cm
Tag4	+5 cm	-3 cm
Commercial tag	+45 cm	-40 cm
Tag Alien	+2 cm	-3 cm

Next, the maximum vertical distance of non-alignment between the tags and the RFID reader antennas is tested. The antennas are placed at a 30 cm distance from the tags, starting from being completely aligned. For tag 4 this distance is only 15 cm since it is the maximum distance at which the tag is readable. The results of this test can be analyzed in table 5.3. The upside distance column indicates the maximum distance at which the antennas are above the tags and that a reading was obtained. The downside distance column indicates the same distance at which the antennas are below the tags. Analysing the results table it can be deduced that the majority of the tags show a higher susceptibility in the case where the reader's antennas are in a lower position. When comparing these results with the free space test results from table 5.1, it can be concluded that the tags that present higher tolerance to misalignment are the ones that present also higher reading distances.

To test another practical scenario where the free space tags could be applied, tags 1 and 2 are now placed on a garment to evaluate the possibility of using these tags as,

for example, access control system, as shown in figure 5.9 . The tags are placed on one arm of the garment, where both this material and the human tissue are affecting the antennas' near filed and influencing its operation. Looking at the results of this test present in the table 5.4, it can be concluded that both tags perform well in this situation.

Figure 5.9: Free space tag applied on cloth.

Table 5.4: Free space tag applied on cloth test results.

Tag	**Maximum read distance**
Tag1	75 cm
Tag2	80 cm

Tag 2 went from a maximum read distance of 1,5 m to 0,8 m, which for an access control application is more than enough. Tag 1, on the other hand, reached a staggering 75 cm, even increasing its read distance when compared to the results of the free space tests in table 5.1.

5.3 Performance of tags on a bottle

As in the previous experiments, tags designed for free space are also considered here to make a comparison between both tag types. Although the antennas were only designed to a certain bottle, other bottles were also considered to evaluate the reading

distance. The bottles considered for these tests are those shown in the figure 5.10.

Figure 5.10: Bottles used for tag testing.

The B bottle, the one in the middle, is the bottle whose dimensions match those used in simulation environment. It is therefore expected that the antennas will behave better when attached to this bottle. A summary of the bottles' dimensions can be seen in the table 5.5.

Table 5.5: Bottle measures.

Bottle	Total Height	Body Height	Radius	Thickness
Bottle A	28 cm	22 cm	6.8 cm	2.01 mm
Bottle B	31 cm	20 cm	7.1 cm	1.98 mm
Bottle C	29 cm	18 cm	6.5 cm	2.08 mm

5.3.1 Empty bottles

First, the bottles are emptied and a test is performed. The tags are placed on the bottles, with tape securing the sides of the paper on which they are printed. With this experiment, the effect that the bottle has on the reading distance of the tags is studied, comparing its results with those of the previous tests. The 5.6 table shows the results obtained from this test.

Table 5.6: Results of the test with tags attached to empty bottles.

3***Tag**	**Maximum read distance**					
	Non-controlled			**Controlled**		
	A	**B**	**C**	**A**	**B**	**C**
Tag1	25 cm	35 cm	40 cm	20 cm	20 cm	10 cm
Tag2	95 cm	85 cm	90 cm	90 cm	28 cm	56 cm
Tag3	170 cm	170 cm	175 cm	176 cm	184 cm	150 cm
Tag4	55 cm	35 cm	50 cm	Not read	Not read	10 cm
Commercial tag	145 cm	145 cm	145 cm	40 cm	20 cm	20 cm
Tag Alien	10 cm	1 cm	5 cm	Not read	Not read	Not read

It is important to highlight that none of the tags were designed for this scenario. Attending to table 5.6 it can be concluded that tag 3, designed for a bottle with liquid, works quite well without the presence of liquid. Its reading distance is 1.8 m when attached to the bottle B. Its performance with the other bottles does not degrade too much, still being able to be read at 1.5 m. It should be noted that, for these more irregular bottles, the tag was placed in the spot with the greatest similarity to the radius of the bottle used in design. The values in the uncontrolled environment do not diverge much from these, with the maximum reading distance being 1.7 m. Tag 4, also dimensioned for a bottle with liquid, always showed worse results when compared with tag 3. Besides practically not having been able to be read in a controlled environment, the values in an uncontrolled environment are not so high as tag 3.

Regarding tags 1 and 2, dimensioned for free space, it is also possible to read them even when placed in an empty bottle. The distances decreased when compared to the free space tests, which is expected. Tag 1 presents lower reading distances than tag 2, as happened in free space also. The same happens with the commercial tag. There is a big difference between the controlled and non-controlled environment tests on these tags, which may mean that with more signal reflections, larger reading distances are achieved. As for the Alien tag, it could only be read in a non-controlled environment, and the distances didn't go beyond 10 cm.

5.3.2 Bottles with water

Next, the bottles are filled with tap water and the same test is performed. The summary of the results are shown in table 5.7. It is clearly noticeable that the introduction of liquid drastically changes the performance of the antennas.

Table 5.7: Results of the test with tags attached to bottles with water.

3***Tag**	**Maximum read distance**					
	Non-controlled			**Controlled**		
	A	**B**	**C**	**A**	**B**	**C**
Tag1	Not read	Not read	Not read	Not read	Not read	Not read
Tag2	Not read	5 cm	Not read	10 cm	12 cm	Not read
Tag3	Not read	Not read	Not read	28 cm	30 cm	Not read
Tag4	Not read	Not read	Not read	Not read	Not read	Not read
Commercial tag	Not read	Not read	Not read	Not read	Not read	Not read
Tag Alien	Not read	Not read	Not read	Not read	Not read	Not read

In the controlled environment, tags 2 and 3 can be read. The fact that tag 2 is readable at 10 cm of distance in this scenario is surprising since this tag is designed for free space. Tag 3, designed for this situation, can be read at a range of almost 30 cm both in the bottle for which it was designed, bottle B, as well as in the bottle A. For bottle C, none of the tags could be read. For the uncontrolled environment only tag 2 is able to be read. However, the read distance at which it was read is only 5 cm.

5.3.3 Bottles with wine

Finally this test is performed changing the liquid in the bottle. Since bottles B and C originally have wine inside, the test is performed for this liquid, in order to evaluate the effect on the performance of the tags. However, when changing the liquid to wine, none of the tags were able to be read in either bottle. For bottle C, no tag was read when it was filled with water, and this remained the case for when it was filled with wine. As for bottle B, tag 3 had reached a reading distance of 30 cm, but when applied to this bottle with wine it could no longer be read.

This behavior is justified by the differences in dielectric properties between water and wine. Figure 5.11 shows the $|S_{11}|$ obtained in simulation for a bottle with wine.

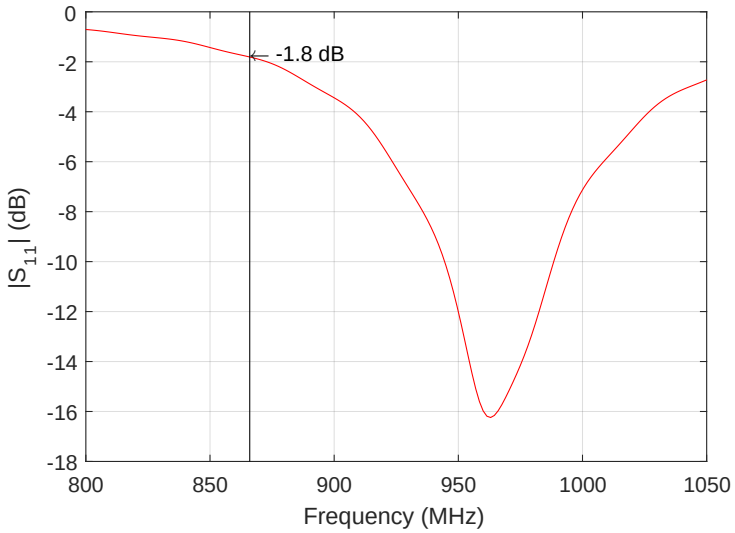

Figure 5.11: $|S_{11}|$ parameter of antenna applied on simulated bottle with wine.

In this simulation the wine was characterized with dielectric properties of ε_R = 74.587 and a loss factor = 26.598 at 200 MHz, as studied in [37]. It is notable in the figure that a is not matched at the desired frequency, showing a value of -1.8 dB at 866 MHz. With the results of this test and simulation it is noticeable that the liquid in the bottle has a great influence on the performance of the tags.

Bibliography

[1] D. Chechi, T. Kundu, and P. Kaur, "The rfid technology and its applications: A review," International Journal of Electronics, Communication Instrumentation Engineering Research and Development (IJECIERD), vol. 2, pp. 109–120, 09 2012.

[2] W. Lumpkins, "Rfid: An evolution of change, from world war ii to the consumer marketplace," IEEE Potentials, vol. 34, pp. 6–12, 09 2015.

[3] "History of rfid technology," accessed on June 2021. https://www.trace-id.com/history-rfid-technology/.

[4] R. Want, "An introduction to rfid technology," Pervasive Computing, IEEE, vol. 5, pp. 25 – 33, 02 2006.

[5] R. S. Dursun Delen, Bill C. Hardgrave, RFID for Better Supply-Chain Management through Enhanced Information Visibility. Production and Operations Management, Volume 16, Issue 5, 2007.

[6] "Epc information," accessed on February 2020. https://www.epc-rfid.info/.

[7] D. Chechi, T. Kundu, and P. Kaur, "The rfid technology and its applications: A review," International Journal of Electronics, Communication Instrumentation Engineering Research and Development (IJECIERD), vol. 2, pp. 109–120, 09 2012.

[8] H. Tizyi, F. Riouch, A. Tribak, A. Najid, and A. Mediavilla, Compact dual-band microstrip antenna for handheld RFID reader. 2015.

[9] "What are the different types of rfid technology?," accessed on February 2020. https://lowrysolutions.com/blog/what-are-the-different-types-of-rfid-technology/.

[10] "Understanding the different types of rfid tags," accessed on February 2020. https://blog.universalrfid.com/types-rfid-tags.

[11] "Uhf rfid frequency regulations," accessed on February 2020. https://www.atlasrfidstore.com/rfid-insider/uhf-rfid-frequency-regulations.

[12] "What's the difference between iso and epc?," accessed on February 2020. https://www.rfidjournal.com/faq/whats-the-difference-between-iso-and-epc.

[13] "Uhf rfid tag communications: Protocols and standards," accessed on February 2020. https://blog.atlasrfidstore.com/uhf-rfid-tag-communications-protocols-standards.

[14] T. Lotlikar, R. Kankapurkar, A. Parekar, and A. Mohite, Comparative study of Barcode, QR-code and RFID System. Internacional Journal of Computer Technology and Applications, 2013.

[15] N. Huber, K. Michael, and L. McCathie, "Barriers to rfid adoption in the supply chain," pp. 1 – 6, 10 2007.

[16] N. Wu, M. Nystrom, T. Lin, and H. Yu, "Challenges to global rfid adoption," Technovation, vol. 26, pp. 1317–1323, 12 2006.

[17] L. U. Toni Björninen, Atef Z. Elsherbeni, Low-Profile Conformal UHF RFID Tag Antenna for Integration With Water Bottles. IEEE Antennas and Wireless Propagation Letters, Vol. 10, 2011.

[18] S. He, Y. Zhang, L. Li, Y. Lu, Y. Zhang, and H. Liu, "High performance uhf rfid tag antennas on liquid-filled bottles," Progress In Electromagnetics Research, vol. 165, pp. 83–92, 01 2019.

[19] J. Xi and T. Ye, "Conformal uhf rfid tag antenna mountable on winebottle neck," pp. 1–2, 07 2012.

[20] Q. Liu, H. Li, and Y.-F. Yu, "A versatile flexible uhf rfid tag for glass bottle labelling in self-service stores," IEEE Access, vol. PP, pp. 1–1, 10 2018.

[21] Z. Hu and P. Cole, "Bottle packaged wine product detection by uhf rfid systems," pp. 301 – 304, 10 2010.

[22] R. Quiroz, A. Thierry, B. Poussot, and J.-M. Laheurte, "Combined rfid tag antenna for recipients containing liquids," Electronics Letters, vol. 49, pp. 240–242, 02 2013.

[23] R. Gonçalves, Desenho de antenas para sensores passivos em materiais não convencionais. Universidade de Aveiro, 2016.

[24] G. Marrocco, "The art of uhf rfid antenna design: impedance-matching and size-reduction techniques," IEEE Antennas and Propagation Magazine, vol. 50, no. 1, pp. 66–79, 2008.

[25] Z. W. Tiling Hu, Caifeng Liu, Design and Analysis of UHF Tag Antenna Structure. IEEE, 2011.

[26] K. Rao, P. Nikitin, and S. Lam, "Antenna design for uhf rfid tags: A review and a practical application," Antennas and Propagation, IEEE Transactions on, vol. 53, pp. 3870 – 3876, 01 2006.

[27] "Cst studio suite," accessed on June 2021. https://www.3ds.com/products-services/simulia/products/cst-studio-suite/.

[28] J. Xi and H. Zhu, "Uhf rfid impedance matching: T-match-dipole tag design on the highway," 2015 IEEE International Conference on RFID (RFID), pp. 86–93, 2015.

[29] S. P. Hae-Won Son, Design of RFID tag antennas using an inductively coupled feed. IEEE, 2005.

[30] "Murata microchip datasheet," accessed on May 2021. https://pt.mouser.com/datasheet/2/281/k70e-1518771.pdf.

[31] L. Yang, A. Rida, R. Vyas, and M. Tentzeris, "Rfid tag and rf structures on a paper substrate using inkjet-printing technology," Microwave Theory and Techniques, IEEE Transactions on, vol. 55, pp. 2894 – 2901, 01 2008.

[32] "The thickness of printing paper," accessed on January 2020. https://www.zxprinter.com/support/paper-thickness.html.

[33] H. Miranda, Sistemas RFID UHF. Universidade de Aveiro, 2015.

[34] "Microchip sl3s1013ftb0 datasheet," accessed on March 2021. https://pt.mouser.com/datasheet/2/302/SL3S1003$_1$013 − 1127858.*pdf*.

[35] "Relative permittivity - the dielectric constant," accessed on January 2020. https://www.engineeringtoolbox.com/relative-permittivity-d$_1$660.*html*.

[36] C. G. Malmberg and A. A. Maryott, "Dielectric constant of water from 0 0 to 100 0 c," 2011.

[37] A. García, J. Torres, M. de Blas, A. Francisco, and R. Illanes, "Dielectric characteristics of grape juice and wine," Biosystems Engineering, vol. 88, pp. 343–349, 07 2004.